ON THE DESIGN AND USE OF A FLEXIBLE NOZZLE FOR THE GALCIT TRANSONIC WIND TUNNEL

Thesis by

Satish Dhawan

In Partial Fulfillment of the Requirements
For the Degree of
Aeronautical Engineer

California Institute of Technology
Pasadena, California

1949

ACKNOWLEDGEMENTS

Deep appreciation is expressed to Dr. Hans Wolfgang Liepmann for directing and supervising this work. His interest and guidance were a constant source of enthusiasm and evaluation. The design and calibration of the flexible nozzle was carried out jointly with Mr. Anatol Roshko. His share of the work is gratefully acknowledged. Mr. Harry Ashkenas' cooperation and advice during the design and experimental work form a valuable contribution. Special thanks are due to Gerry Ellis for her excellent typing.

ABSTRACT

Some aspects concerning the design of flexible nozzles for use in supersonic wind tunnels are discussed. Methods are investigated for matching the deflection patterns of nozzle plates and the theoretical aerodynamic shapes required for uniform, parallel, shock-free flow. Application of the design procedures to the Galcit 4" x 10" transonic wind tunnel is detailed. As a demonstration of a use of the tunnel, the Mach number of shock detachment from a 10° wedge (half angle) is experimentally investigated.

TABLE OF CONTENTS

INTRODUCTION

Towards the beginning of 1948 it became necessary to redesign the entire test section and the diffuser of the Galcit 2" x 20" transonic wind tunnel. The reasons for the redesign (Ref. 1, p. 6) are associated with the developments in the research program pertaining to the experimental investigation of the boundary layer and shock wave interaction phenomenon in supersonic flow.

One of the features the new design called for was the production of easily controlled, uniform, shock free supersonic flow. The use of a flexible nozzle was a logical answer to this requirement. The idea of using such a nozzle is not new and no originality is claimed on this account. However, no description of such a design appears to have been published. This work reports on some of the design considerations that govern the successful use of flexible nozzles. In particular, it details the investigations bearing on the nozzle designed for the Galcit 4" x 10" transonic tunnel. A record of the performance of this design is also given.

Part I is a general, qualitative discussion concerning the design of flexible nozzles for uniform supersonic flow. Part II consists of some notes on the flexible nozzle designed for the Galcit 4" x 10" transonic tunnel and on the production of required flows in the tunnel. Part III exhibits a use of the tunnel in investigating the shock detachment from a wedge.

PART I

DISCUSSION OF DESIGN PROCEDURES

1. A supersonic wind tunnel capable of operating over a range of Mach Numbers must employ either a series of fixed geometry nozzles or employ some other device for obtaining changes in nozzle geometry and shape over the range of operation. The use of the flexible nozzle plate in achieving this purpose is discussed here with special reference to small wind tunnels.

A flexible nozzle for producing supersonic flow must fulfill the following requirements:

(a) It must be capable of continuously changing the area ratio

$$\frac{A}{A^*} = \frac{1}{M}\left\{\frac{2+(\gamma-1)M^2}{\gamma+1}\right\}^{\frac{\gamma+1}{2(\gamma-1)}} \qquad \text{(Ref. 2 p. 34)}$$

throughout the range of the test section Mach Numbers, where A is the test section area, A* the throat area, and M the test section Mach Number.

(b) The nozzle contours must continuously correspond to the aerodynamic shapes* necessary for the production of uniform, parallel shock-free flow in the test section.

These fundamental considerations affect all other features influencing the design of flexible nozzles. For example, the second requirement dictates the physical design of the nozzle plate by setting a limit to local distortions since disturbance free flow

---

* By aerodynamic shape is meant, in general, the theoretical shapes given by two dimensional supersonic flow theory including a correction for boundary layer growth on the nozzle walls.

necessitates a close reproduction of the theoretical shapes.

2. The flexible plate nozzle, as used in supersonic wind tunnels achieves the desired speed changes in the test section by reproducing the wall contours and area ratios associated with the required flows with its deflection patterns. The wind tunnel being two-dimensional, the nozzle plate is of uniform width and very frequently of uniform cross-section.

In general, there may be distinguished a basic procedure available for obtaining arbitrary contours for the sides of the nozzle from such a plate as is mentioned above. In this procedure, elastic deformations of the plate produced by suitable conditions of loading, are used to obtain the required shapes. Within this general procedure specific designs may choose from a variety of means to achieve the object. For instance, one design may force the plate at a large number of points to assume prescribed positions.* While another** may so choose to locate a few loads that their magnitudes, when properly proportioned, produce a natural deflection pattern of the plate conforming to the one desired. Yet other designs may use combinations of the above two schemes.***

One other possible device may be mentioned here. The curvature of a plate (or beam) is inversely proportional to the moment of inertia of its cross-section

---

* This method of obtaining flexible nozzles for supersonic flow has been used, for example, in the $2\frac{1}{2}$" x $2\frac{1}{2}$" Galcit supersonic tunnel.

** The Galcit 4" x 10" transonic tunnel incorporates this design.

*** e.g., the 12" x 12" supersonic tunnel at J.P.L. C.I.T.

$$\frac{d^2y}{dx^2} \sim \frac{1}{I}$$ where y = deflection, $\frac{d^2y}{dx^2}$ = curvature & I = moment of inertia

For a plate of uniform width (as in the case of two-dimensional tunnels) and rectangular cross-section this becomes

$$\frac{d^2y}{dx^2} \sim \frac{1}{d^3}$$ where d = thickness of plate;

so that a depth or thickness variation may be used in producing variations in the deflection curves. There are however obvious mechanical difficulties preventing any extensive use of this feature in practice.

3. In order to systematize a design procedure for obtaining nozzle shapes from the deflection patterns (or a combination of patterns) of a flat-plate it is necessary, first, to study the general characteristics of the aerodynamic shapes which are to be produced.

Theoretically, it is well known that uniform sonic flow in a channel may be converted into flow at higher speeds by an expansion process involving increasing areas of the channel — the increase in speed being a function of the area ratio alone. The problem of determining the actual shape of the nozzle walls becomes pertinent only when a parallel, shock free flow is desired in a section of the channel. It is then found that apart from a unique area ratio associated with the desired Mach number the actual contour of the nozzle, i.e., the manner in which the expansion is produced, also vitally affects the character of the flow in the section. The simplest form of nozzle shape for parallel, uniform shock free flow would consist in employing the simplest form of expansion, namely, around a sharp corner. This results in the well-known Prandtl-Meyer flow around a corner. The nozzle contour subsequent to the expansion would then be determined by a system of two-dimensional characteristics according to the method due to Busemann (or other equivalent methods), employing appropriate turns in the wall to cancel the system of waves originating at the corner. A nozzle designed on this principle is illustrated in Fig. 1.* In actual practice such a design is not to be recommended for the following reasons:

(1) Nozzles designed with a sharp corner at the throat are liable to be extremely sensitive to errors in design arising out of inherent indeterminacies like boundary layer growth or other inadequate assumptions regarding design parameters.

(2) It is impossible to obtain an ideally sharp corner due to the presence of boundary layer. Also, mechanically speaking the adaptation of this type of design for flexible nozzles is not attractive.

(3) Separation at the corner.

The conventional method generally used for nozzle shapes is to obtain the initial expansion by means of a smooth curve (equivalent to spreading out the sharp corner). The shape of this curve is generally assumed** (for example, a circular arc). The subsequent nozzle contour then may be determined by any of the standard methods, e.g., graphical construction(Ref. 4)or by equivalent analytical methods

---

* An application of such a nozzle is discussed in Ref. 3.

** There are special cases in which it has been attempted to compute the coordinates of this initial expansion curve. See, for example, Ref. 3. However, these do not afford any general procedure.

Ref. 5. The graphical method is considered to be quite adequate for a comparatively low range of Mach numbers (especially so because of the non existance of rational, general, methods of determining boundary layer growth and effects of the inlet shape in the contraction section leading up to the throat). For a higher speed range, the analytical method is to be preferred in view of its greater accuracy and also because it affords a priori means of estimating the length of the nozzle.

The essential features of the aerodynamic curves obtained by following the procedures outlined above and which affect the design of the flexible nozzle plate may be summarized as follows:

(1) The initial expansion region consists of a relatively short length (compared to the total length of the nozzle) with relatively high curvature. The curvature of this portion increases with increasing final Mach number for nozzles of fixed overall length and belonging (approximately) to a continuous family. (See Fig. 2.)

(2) The portion of the nozzle immediately following the initial expansion has small curvature and contains an inflexion point (reversal in sign of the curvature). Graphically constructed nozzles show this region as a straight segment, the center of which may be referred to as the inflexion point. In actual design work, a smooth curve is used through the points obtained by the construction. The inflexion point location shifts with nozzle shapes designed for different Mach numbers, in general moving closer to the throat for nozzles of constant length and increasing M.

(3) The final or terminal section of the nozzle has the greatest length and a uniformly decreasing curvature.

(4) The nozzle shape coordinates are functions of the flow Mach number, the Prandtl-Meyer angle associated with the flow and the chosen expansion angle for the initial expansion (equal to or less than, half the Prandtl-Meyer angle). In general the shapes are not linearly related for varying Mach numbers.

In addition, it might be mentioned that the over-all length of the nozzle is controlled by choice of the total initial expansion angle (equal to the nozzle wall slope at the inflexion point) which according to two-dimensional supersonic flow theory must be less than or at the most equal to one half the Prandtl-Meyer angle associated with the flow in question. The length of the center portion (with low curvature containing the inflexion point) is a function of the curvature of the initial portion producing the expansion being a minimum when the initial curve is shrunk to a point. Typical nozzle shapes for the Mach number range up to 1.5 are shown in Fig. 2. They show the features discussed above. The curvatures for a representative case of $M = 1.365$ are shown in Fig. 3.

4. To form an idea of the shapes of the plate deflection curves in relation to the aerodynamic shapes, one may now consider the deflection patterns of a simply-supported uniform beam under the action of a single concentrated load (Fig. 4). The main feature of the deflection pattern of such a system in contrast to the aerodynamic shapes is that there is no reversal in curvature in the deflection

curve. Also the changes in shape that may be produced in such a system by varying the load are all linearly related (deflection being a linear function of the load). These considerations at once point to the necessity of changing the end conditions and or loading for producing the change in curvature. It becomes apparent that multiple loads or changes in location of individual loads, or perhaps combinations of the two, will be required to accomplish the desired shifts in inflexion point and reproduction of the required shapes for different flows. One may now proceed to discuss the means available in regard to systems of loading and end conditions for the plate for the purpose at hand. Evidently, one solution is to provide a sufficient number of jack points on the plate so that the plate ordinates can be made exactly equal to those required for the aerodynamic curve at a finite number of points. Spacing of the jacks would be dictated by consideration of local deflections. This method of producing nozzle shapes is employed in the 12" x 12" supersonic wind tunnel at the Jet Propulsion Laboratory C.I.T. The coordinates of the resulting plate shape at all other points, after positioning of the jacks, are ascertained by relaxation methods of analysis (Ref. 5). Any discrepancies in wall shape and the aerodynamic curve show up as pressure or flow inclination errors in the observed test section flow. These may be corrected by the procedure discussed in Ref. 5 and briefly outlined in Part II of this work. In this method of producing nozzle shapes a considerable number of jacks have to be used for attaining a high degree of accuracy. The arrangement is relatively complex on account of the nature of the problem and seems quite necessary for wind tunnels of this range and accuracy. For wind tunnels of a lower and narrower range (up to $M = 1.5$), a somewhat simpler and comparatively easily constructed arrangement may be contrived. In this, the ends of the plate are direction-fixed* for obtaining the reversal in curvature (Fig. 5). A minimum of two jacks may be used and means investigated by which the deflection curves match the aerodynamic shapes closely. The low range of Mach numbers in the case of the Galcit 4" x 10" transonic tunnel warranted such a choice. The earlier mentioned device of change in thickness of the plate was used, in addition, for improvement of the deflection shapes. Of course a thickness variation -- in view of practical considerations -- may be used to produce only one closely matching shape. For other shapes, the discrepancies would have to be taken care of by suitable jack adjustments.

During the course of designing the flexible nozzle for the Galcit 4" x 10" tunnel, an attempt was first made to determine mathematically, in quite general terms, the optimum positioning, type and magnitude of loadings in order that the deflection pattern of a flat plate may reproduce closely quite arbitrary shapes over a limited range. As a simplified approach the problem was set up as a beam problem with known end conditions (direction fixed in this case) and known loadings (in the form of point loads). The control variables would then be the location and the magnitude of the loads,

---

* Fixing one end and making the other pin-jointed would have the same general result, but this method is less suitable for mechanical reasons associated with securing smooth entrance and exit conditions for the flow.

the constraints appearing as prescribed shapes for the deflection curves. It became clear during this investigation that although the problem posed had a possible solution, the time and effort required for a general solution adaptable for the practical needs of design would of necessity delay progress in design of the nozzle for the tunnel. In view of these considerations, some of the less important variables were eliminated either by physical reasoning or trial and error methods. As a simplification to the above stated problem, it was decided to fix the number and form of loads to two concentrated loads. The location* was restricted to specific points on the plate. Part II of this work deals in the main with the investigations into solutions of the simplified problem. It also contains some notes on the methods employed during design of the nozzle.

---

* Practically, it would be extremely difficult to provide movable loads on the plate.

PART II

DESIGN NOTES AND MATCHING PROCEDURES FOR THE

GALCIT 4" x 10" TRANSONIC WIND TUNNEL

1. General

For reasons of simplicity, it was decided to use a one-wall flexible nozzle for the production of supersonic flow. This choice facilitated the incorporation of an enclosed traversing mechanism* operating through a slot in the straight (top) wall of the tunnel; at the same time, the ease of control during operation was doubled.

2. Aerodynamic Shapes

Theoretical nozzle shapes were designed for six Mach numbers covering the range $M = 1$ to $M = 1.5$. The coordinates of the nozzle contours for the various Mach numbers were obtained graphically by the method of characteristics as presented in Ref. 4. The nozzle expansion angle (the angle made by the nozzle wall with the nozzle axis at the point of inflexion) and the number of reflected waves were so chosen that the resultant nozzle length remained constant throughout the design range. It was desirable to obtain aerodynamic shapes which belonged to a continuous family. The graphical method of design does not lend itself too well for such manipulations and as seen in Fig. 2. The aerodynamic shapes do not fulfill this requirement. However, they are of the same over-all length (throat to exit). The nozzle contours obtained by the method of characteristics do not incorporate the

---

* Ref. 1. p.12.

growth of boundary layer on the walls of the tunnel. It is usual to correct for this by displacement of the walls. In the present case a simple linear correction of 0.021" per inch was allowed for the boundary layer on the basis of experience in the 2" x 20" test section. The low range of Mach numbers serves to make this allowance a reasonably good one. Test section surveys reveal no serious effects due to boundary layer growth; furthermore, it is possible in the present design to vary the correction for boundary layer (Ref. 1, p. 9) and so improve the flow.

3. Nozzle Plate and Control Configuration

The specifications of the tunnel called for a flexible nozzle which would give a continuous variation in Mach number up to $M = 1.5$ in the supersonic speed range. (For the subsonic range of operation a flexible second throat was used with the main nozzle undeflected.) For reasons of simplicity in use and construction, it was desirable to keep the number of controls on the flexible plate to a minimum. At the same time, the controls had to be sufficient to satisfy the minimum requirements for the production of the aerodynamic shapes for parallel, shock free flow. The nozzle plate finally adopted for the tunnel is shown in Fig. 6. It is effectively* 36 inches in length and 4 inches wide and varies in thickness as shown.** The jack positions

---

* Actually, the plate is continued for 9 inches beyond the downstream fixed end — this portion forming part of the test section.

** The details of the mechanical design and fabrication of the flexible nozzle plate are contained in Ref. 1, pp. 37-41.

were dictated by considerations of approximating the aerodynamic shapes and the over-all test section length. The latter consideration affects primarily the location of the throat and hence that of the main jack. The range and closeness of reproduction of the aerodynamic contours controls the location of the second jack. Several trials were made for determining the optimum location of the second jack by observing the maximum discrepancy in ordinates and slopes between the nozzle elastic and aerodynamic curves over the range of operation. An auxiliary control in the form of a moment arm was provided in the center of the nozzle plate. As observation of the deflection shapes with two jacks showed, for some settings, the relative error distribution between the desired and the obtained shapes was almost symmetrical about the aerodynamic shape as a mean (for instance, see Fig. 10). It was felt that an appropriate addition or subtraction of the deflection curve furnished by a pure moment could be used to advantage in bringing the two shapes still closer* together. A comparative study of the aerodynamic shapes and the elastic curves of a plate with uniform thickness showed that, in general, over the desired range the aerodynamic curves had a greater curvature immediately down stream of the throat than could be obtained by a plate with such a uniform moment of inertia distribution. A step variation in thickness of the plate served to give the greater curvatures desired in this region.

---

* Subsequent analysis showed that the use of the moment arm control was much less effective than expected. It's use was confined only to a very small range of changes in the shapes.

(Actually, a smooth transition curve was used to avoid stress concentrations in the plate.) The location of the "step" was determined by trial.

4. Matching Procedures

Having decided on the number and form of the shape changing mechanisms, it was then considered desirable to obtain some procedure for actually producing desired nozzle shapes for uniform flow, i.e., setting the jacks. One obvious method available was to experimentally determine the jack positions for each aerodynamic shape by measurement of the ordinates (using, for instance, a dial gage) at a number of locations. Such a procedure is however, always open to experimental errors, and it was considered more desirable to attempt to determine the control settings, a priori, by systematic calculation.

Some general remarks in matching the deflection and aerodynamic shapes are in order here. In general, if the curvatures of the aerodynamic shapes and the moment distribution of the plate are matched, an improved matching of the deflection curves (obtained by two integrations) may be expected. Also, the discrepancies between the first integral of the plate curvatures, i.e., the slopes and slopes of the aerodynamic curve, would afford an idea of where to expect disturbances in the flow (since small changes in slope of the nozzle bear a direct relation to the pressure disturbances propagated in the flow). This provides a means for determining the location of corrections in the wall slope from flow observations.

In Ref. 6 a general method was suggested for the correction of nozzle jack positions from observed flow errors. For the sake of completeness, this method is briefly reviewed here. From observations of the pressure disturbances and flow inclinations in the test section the locations of the slope errors in the plate are determined. Knowing the slope influence curves* for jack displacements, a correction may be worked out for the appropriate jacks on the following principle:

If $\epsilon_i(x)$ is the slope influence function of the ith control, then the composite function describing the resultant slope change due to movements a_i of the controls is

$$\Sigma' = \sum'_{i=1,2\ldots n} a_i \epsilon_i(x)$$

The best correction then would be one where the a_i's satisfy the following relation

$$\frac{\partial}{\partial a_i} \int_{x_0}^{x_1} \left[f(x) - \sum'_{i=1\ldots n} a_i \epsilon_i(x)\right]^2 dx = 0$$

where $f(x)$ is the exact correction, n the number of controls, and the limits of integration cover the region of the flow affected by the change. The above principle of least squares results in n simultaneous, linear equations involving the unknown a_i's. This principle of least squares may be employed to obtain jack settings in the first place, for the case in hand, where i = 1, 2, 3. However, it turns out that such an application of this principle while raising several subsidiary problems does not give even moderately fair results. In the first place, the advantage of matching the curvatures or slopes in preference to ordinates may no longer be employed. This is on account of the fact that the "fit" provided by the "least squares"

---

* An influence curve is one which indicates changes in the dependent variable all over a range due to unit change in the independent variable.

process is the best possible in this sense and cannot be improved upon by any process of integration. As a matter of fact, an integration of the slopes which have been matched by this principle may make worse the discrepancies in the ordinates. A second problem posed is as follows: the criterion of minimizing the square of the error distribution in ordinates, if used to obtain control settings, does not guarantee that the resultant deflection shape will provide the required area ratio for a given test section Mach number. This is due to the fact that once the a_i's are determined the maximum of the resultant shape has to be accepted in magnitude and location. This difficulty may be overcome by a design employing movable nozzle walls which provide subsequent readjustment for the area ratio. This was not possible for the transonic tunnel. In addition to the above difficulties, a trial matching based on the least squares method showed that its use was not justified. Fig. 7 shows the deflection shape obtained by this method in comparison with the desired aerodynamic curve for $M = 1.365$. The wavy pattern of the plate is clearly unsuited for the production of uniform flow. Also the jack deflections for the above shape proved to be excessive for a safe loading of the plate material.

In view of the above observations, an alternative procedure for matching nozzle shapes was developed using the two main controls only, namely the jacks. Stated in a simplified form, this method essentially seeks a solution to the following problem: Given a fixed ended beam of known thickness distribution and loaded with two point loads, W_1 and W_2, at known locations. What combination of W_1 and W_2 will produce a prescribed maximum in the deflection shape of the beam and at the same time closely reproduce a given function (the aerodynamic shape) over a part of its length? The restriction on the maximum is necessary because of the uniqueness of the area ratio $\frac{A}{A^*}\left(=\frac{h}{h^*}\right)$ associated with a desired Mach number in the test section.

Let $y_1(x)$ and $y_2(x)$ be the deflection influence curves for the loads W_1 and W_2 for their respective locations (i.e., curves describing the deflection of the plate everywhere with unit W_1 or W_2).

The resultant elastic shape is then,

$$y = y(W_1, W_2, x) = W_1 y_1(x) + W_2 y_2(x) \tag{1}$$

The location of the maximum of this curve X_m may be obtained by solving the equation

$$\frac{dy}{dx} = 0 \tag{2}$$

This gives X_m as a function of the loads W_1, W_2 and may be expressed as

$$X_m = \phi(\upsilon)$$

where $\upsilon = \frac{W_2}{W_1}$, ratio of the loads at the jack points (3)

The magnitude of the maximum ordinate may be obtained from equation (1),

$$y_m = \psi(W_1, W_2, X_m) \tag{4}$$

Since y_m is fixed by the area ratio $\frac{A}{A^*} = \frac{h}{h^*}$ where h = test section height and h^* = height at the critical section. We may write equation (4) as

$$K_1 W_1 + K_2 W_2 = y_m \tag{4a}$$

where K_1 = a function involving the first jack influence curve and X_m

K_2 = a function involving the second jack influence curve and X_m

Using $\frac{W_2}{W_1} = \nu$ we obtain

$$\left.\begin{aligned} W_1 &= \frac{y_m}{K_1 + \nu K_2} \\ W_2 &= \frac{\nu y_m}{K_1 + \nu K_2} \end{aligned}\right\} \qquad (5)$$

The unknown loads W_1 and W_2 are thus expressed as functions of the desired throat height, nozzle influence curves, and the parameter ν (the load ratio). This enables a chart of the form shown in Fig. 8 to be drawn, showing the possible nozzle shapes having the same maximum with ν as the parameter. A value of ν designating the shape which best fits the aerodynamic curve and provides the required area ratio may now be picked and the corresponding control positions computed.

Using this procedure, control settings were worked out for the following test section Mach numbers: M = 1.503; 1.435; 1.365; 1.294; 1.217; and 1.133. Figs. 8 through 13 show the matched aerodynamic and elastic shapes over this range. The maximum discrepancy in ordinate in these is approximately 2.5 per cent. Fig. 14 shows curves which may be employed for obtaining control settings for intermediate values of M in the operating range of the tunnel.

5. Test Section Surveys

For the purpose of evaluation and calibration, a series of Mach number surveys were made of the test section of the tunnel at the calculated control settings. The surveys were made by means of a circular duralumin plate with a row of radially located (0.0135 inch dia) pressure holes spaced at intervals of ½ inch. The circular plate took the place of one of the regular glass windows in the sides of the tunnel with its center approximately in the same location as the center of the 10" x 10" test section. The plate could be rotated to obtain distributions both normal and parallel to the flow direction. The pressure holes were connected to the Mach meter (described in Ref.7) through a manifold switch. The vertical surveys would show, in the main, disturbances arising from the nozzle plate while the horizontal surveys would reveal those originating at the side walls of the tunnel. Figs. 15 and 16 show the Mach number distributions over the supersonic operating range of the tunnel for the horizontal and vertical directions, respectively.

The vertical distributions indicate considerably greater uniformity of flow as compared to that in the horizontal direction. The maximum variation of M in the vertical direction over the operating range is about $\pm$ 0.5 per cent from the mean as compared to approximately $\pm$ 2 per cent in the horizontal direction. The greater non-uniformity in the horizontal direction is due to slight leakage at the joints in the sectioned* side walls of the tunnel. Careful sealing decreased the magnitude of the variations without shifting their locations. For very smooth flows, the use of continuous panels for the sides of the tunnel should render the horizontal variations quite negligible.

The test section surveys presented in Figs. 15 and 16 were all conducted with the same boundary layer correction** with the exception

---

* The tunnel walls were made in sections to enable changes in location of the windows. See page 9 of Ref. 1.

** (.021 inches per inch)

of the $M = 1.5$ survey. The surveys reveal small over-all gradients and also show that the average test section Mach numbers differ by small amounts from that indicated by the calculated control settings. These discrepancies and some suggestions for minimizing them are discussed in order:

The small over-all gradients in the test section are believed to be mainly due to inaccuracies in the boundary layer correction. Changing the allowance for boundary layer by shifting the position of the lower wall effectively improved the flow in the test section. Figs. 17(a) and 17(b) show test section surveys for $M = 1.5$ with different settings of the lower wall. It will be noticed that Fig. 17(b) shows a marked improvement of distribution over Fig. 17(a). The gradient has been eliminated and the magnitude of the variations decreased.

The deviations of average test section Mach numbers from that indicated by the control settings are due to slight differences in the area ratio. These are caused mainly by the shift of the lower well when an allowance is made for the boundary layer. A further cause for these small discrepancies is the aerodynamic loading on the plate which produces slight changes in the deflection shape of the plate causing shifts in the throat height. The upper and lower surfaces of the nozzle plate are vented to each other around the sides. It was expected that when steady conditions were attained, the aerodynamic pressure on the two surfaces would equalize. Actually, the venting seems to be imperfect, and there exists a small pressure differential between the two surfaces. If the moment arm (near the center of the plate) is left unclamped, a slight deflection may be noticed in the plate when the flow is established. The effect of this deflection on the shapes of the plate used in matching the aerodynamic curves is negligible at the lower Mach numbers. At $M = 1.5$, however, the deflection (approximately 1/16 inch) was sufficient to cause a noticeable change in the flow. Clamping the moment arm with the tangent screws, after the main controls were set, effectively eliminates the deflection. The test section survey for this Mach number was made with the moment arm clamped.

In conclusion it may be remarked that in experimental work, of the type the tunnel is designed for, the measurement and attainment of absolute values of quantities is not nearly so important as the relative ones. Uniformity of flow in the test section is thus of far greater importance than achieving an absolute level of velocity or pressure. It is felt that the present design of the flexible nozzle achieves this criterion to a reasonable degree together with the provision of an easy and continuous control of the Mach number.

PART III

EXPERIMENTAL INVESTIGATION OF THE DETACHMENT MACH NUMBER FOR A 10° (HALF ANGLE) WEDGE

1. Aim

The purpose of this section is to serve as a demonstration of the use of the flexible nozzle described in the earlier sections. The results of the investigation are believed to be of some general interest.

For a given wedge in two-dimensional supersonic flow, there is a minimum Mach number $M_{min} > 1$, predicted by theory, for which an oblique plane shock exists and is attached to the nose of the wedge. For values of M less than M_{min} and greater than 1, there are no flow solutions giving an attached shock wave. For such cases, a detached head wave forms in the flow ahead of the wedge. This shock wave has the general characteristics of being normal to the flow direction at the line of symmetry and becomes more oblique on either side of it. The aim of the experiment reported here was to determine the Mach number of attachment (or detachment) for a 10° wedge (half angle) and compare the result with the theoretical value.

2. Procedure

The wedge (described in a later section) was supported in the tunnel as a cantilever from one of the side window discs so that the nose was approximately half way across the glass section of the window (Figs. 23 and 24). After establishing supersonic flow in the tunnel, the wedge was set at zero angle of attack by equalizing the pressures on its two surfaces (as indicated on a micro-manometer connected to pressure orifices on the upper and lower surfaces of the stem of the wedge). The Mach number of the flow was then continuously lowered by jacking the nozzle down until the shock detached and stood ahead of the wedge. A series of Schlieren spark photographs (e. g., Figs. 25 and 26) were then taken with the detached shock at various distances from the nose of the wedge. At the same time, the Mach number upstream of the detached wave was determined* on the Mach meter (Ref. 7) connected to two pressure orifices in the tunnel top wall ahead of the shock. The distance of the shock, δ, from the nose was determined for each flow speed from enlarged projections of the photographs. A plot of the distance** δ versus the Mach number would then determine the Mach number of detachment for $\delta = 0$. (See Fig. 27)

3. Conclusion

The detachment Mach number (Fig. 27) for a 10° (half angle) wedge, as determined by this experiment, is between 1.41 and 1.44 {see (a) below}. This determination approximately checks the theoretical value of 1.42. The check may not be considered to be very precise or accurate on account of the following reasons:

---

* As a further check, the control settings for the nozzle were noted and the runs repeated at the same settings without the wedge in the tunnel but with the duralumin calibration disc in the side wall covering the location of the wedge. The results of this check, however, proved unsatisfactory. The changed conditions, believed principally due to changes in leakage at the side wall joints, rendered the readings unreliable.

** δ is plotted in the form of a dimensionless ratio $\frac{\delta}{b}$, where $b =$ thickness of the wedge stem; this served as a convenient reference for various magnifications of the Schlieren pictures.

(a) It was impossible, in this experiment, to determine exactly the actual detachment or attachment of the head wave from the wedge nose. As may be expected, due to the presence of boundary layer, there is a fundamental discrepancy between the process of attachment of a shock to a body in supersonic flow as described by inviscid compressible fluid theory and the actual phenomenon in real fluids. The asymptotic approach of the shock to the nose of the wedge and the growth of the shock thickness, relative to the distance, render the ordinary meaning of attachment quite inadequate. Viscous effects, neglected by the inviscid fluid theory, would be extremely important in this process. Noting the similarity to boundary layer thickness definitions, useful integral representations of the process of attachment of a shock to a pointed body may be possible. Theoretical work on this phase should lead to interesting results.

(b) There is some indeterminacy (of the order of $\pm$ 1%) in the measurement of the local Mach number just ahead of the detached shock. The two pressure orifices, located approximately 2 inches and 4 inches, respectively, from the wedge nose (Fig. 27), show a small discrepancy. This is probably due to the combined effects of the shock wave on the boundary layer and the small waves off the joints in the side walls.

In conclusion, it is noted that the convenient and continuous control on the flow provided by the flexible nozzle is an indispensible part of investigations such as the one reported here.

Note on Wedge Design:

The wedge used for the foregoing investigation is shown in Fig. 23. The following points are of interest:

(a) Blocking Thickness

The blocking area* of this wedge is well below (approximately 60 per cent) the minimum necessary to permit the start of supersonic flow. Even so, due to wake blocking effects, it was sufficient to choke the tunnel for Mach numbers close to the detachment Mach number of the wedge. As a remedy, a favorable pressure distribution over the wake of the wedge was used. This was obtained by creating an expansion in that region. One-inch ceiling blocks were used as shown in Fig. 24. Pressure distribution surveys showed that the effect of this change in aspect ratio of the tunnel on the flow was negligible, except to change the mean Mach number of the flow as indicated by the control setting of the nozzle. Since the speed measurements were made independently of the control settings, this proved no drawback.

(b) Side Wall Boundary Layer Effects

The wedge has a span less than that of the tunnel. Earlier work with a wedge spanning the tunnel showed that due to side wall boundary layer interaction effects** Schlieren photographs showed fan-like regions ahead of the plane shock waves from the wedge. A reduction in span resulted in sharply defined waves.

(c) Wedge Nose Length

The nose length of the wedge is designed so that the subsonic region behind the detached shock does not extend to the upper and lower walls of the tunnel. The expansions around the shoulders of the

---

* As determined from Ref. 8, Fig. 3.

** Pointed out by Mr. Morton Alperin

wedge are utilized to accelerate the flow near the walls to supersonic. For a previous design of twice the nose length, it was impossible to obtain smooth attachment or detachment of the shock from the nose. With the present design the head wave may be attached or detached continuously.

APPENDIX I

CALCULATIONS FOR MATCHING THE AERODYNAMIC AND ELASTIC SHAPES

The deflection influence curves for the nozzle plate are given by

(I) Jack Number 1

$$y_1 = \begin{cases} a_2 x^2 + a_3 x^3 & 0 \leq x \leq 8 \\ b_0 + b_1 x + b_2 x^2 + b_3 x^3 & 8 \leq x \leq 12 \\ c_0 + c_1 x + c_2 x^2 + c_3 x^3 & 12 \leq x \leq 36 \end{cases} \qquad (1)$$

(II) Jack Number 2

$$y_2 = \begin{cases} a_2' x^2 + a_3' x^3 & 0 \leq x \leq 12 \\ b_0' + b_1' x + b_2' x^2 + b_3' x^3 & 12 \leq x \leq 27 \\ c_0' + c_1' x + c_2' x^2 + c_3' x^3 & 27 \leq x \leq 36 \end{cases} \qquad (2)$$

where the constants (for y in inches and one-pound loads at the two Jack points) are given by:

$a_2 = 3.026 \times 10^{-4}$	$a_2' = 5.460 \times 10^{-5}$
$a_3 = -2.080 \times 10^{-5}$	$a_3' = -2.850 \times 10^{-6}$
$b_0 = -1.369 \times 10^{-2}$	$b_0' = 1.787 \times 10^{-3}$
$b_1 = 5.150 \times 10^{-3}$	$b_1' = 7.270 \times 10^{-5}$
$b_2 = -3.410 \times 10^{-4}$	$b_2' = 5.470 \times 10^{-6}$
$b_3 = 6.000 \times 10^{-6}$	$b_3' = -2.860 \times 10^{-7}$
$c_0 = 1.190 \times 10^{-2}$	$c_0' = -5.088 \times 10^{-2}$
$c_1 = 1.210 \times 10^{-4}$	$c_1' = 5.914 \times 10^{-3}$
$c_2 = 3.420 \times 10^{-5}$	$c_2' = -2.109 \times 10^{-4}$
$c_3 = 6.000 \times 10^{-7}$	$c_3' = 2.387 \times 10^{-6}$

The combined deflection curve with W_1 and W_2 as the respective loads on the two jacks is

$$y = W_1 y_1 + W_2 y_2 \tag{3}$$

The point of maximum deflection (corresponding to the throat in the nozzle) will be located at some intermediate position between the jack points. By requiring that the maximum should occur as close to the first jack as possible, we need investigate only those combinations of W_1 and W_2 which cause the maximum to occur in the panel $8 \leq x \leq 12$. Differentiating eq. (3) and setting $\frac{dy}{dx} = 0$

$$\left(\frac{dy}{dx}\right)_{x=x_m} = \left\{ 3(W_1 b_3 + W_2 a_3')x^2 + 2(W_1 b_2 + W_2 a_2')x + W_1 b_1 \right\}_{x=x_m} = 0$$

$$\therefore \quad x_m = \frac{-(b_2 + v a_2') \pm \sqrt{(b_2^2 - 3b_1 b_3) - v(3b_1 a_3' - 2b_2 a_2') + (a_2' v)^2}}{3(b_3 + v a_3')}$$

i.e.,

$$x_m = \phi(v) \tag{4}$$

where $v = \frac{W_2}{W_1}$ ratio of the Jack loads (5)

Equation (4) is plotted in Fig. 18. The maximum ordinate of the deflection curve is given by

$$y_m = (W_1 b_3 + W_2 a_3')x_m^3 + (W_1 b_2 + W_2 a_2')x_m^2 + W_1 b_1 x_m + W_1 b_0 \tag{6}$$

This may be written as

$$K_1 W_1 + K_2 W_2 = y_m \tag{7}$$

where $K_1 = b_0 + b_1 x_m + b_2 x_m^2 + b_3 x_m^3$

and $K_2 = a_2' x_m^2 + a_3' x_m^3$

Equations (5) and (7) give

$$W_1 = \frac{y_m}{K_1 + \vartheta K_2} \qquad W_2 = \frac{\vartheta y_m}{K_1 + \vartheta K_2} \tag{8}$$

In order to facilitate rapid calculations, the factor $K_1 + \vartheta K_2$ is plotted as a function of the load ratio ϑ in Fig. 19. The procedure in matching nozzle shapes then consists of the following steps:

(a) The ϑ curves are drawn on an exaggerated scale with corresponding to the throat height of the nozzle shape being matched. (See Fig. 8 for an example of matching for M = 1.5.)

(b) The value of ϑ is determined giving the best approximation to the aerodynamic shape.

(c) X_m is obtained corresponding to this value of ϑ from equation (4). (Fig. 18)

(d) W_1 and W_2, the jack loads, are now calculated from equation (8) with y_m = throat height required.

(e) The jack settings are given by equation (3) with $X = 8$ and $X = 27$ for jack number one and jack number two, respectively.

Fig. 8 shows a complete set of the ϑ curves for M = 1.504. Figs. 9 through 13 show the aerodynamic curves and the corresponding matched elastic curves for M = 1.435, 1.365, 1.294, 1.217, 1.133. Table 1 gives the control settings for these design Mach numbers.

APPENDIX II

ANALYSIS OF NOZZLE PLATE

The form of the nozzle plate adopted for the 4" x 10" Galcit transonic tunnel and the representation as a fixed-ended beam used for analysis is shown in Fig. 6.

The fundamental considerations governing the analysis of beams with direction-fixed ends and variable moments of inertia are:

(a) The total change in slope over the length of the beam is zero,

(b) The total change in level between the supports is zero.

For a beam of given distribution of the moment of inertia $I(x)$, these conditions are sufficient to solve the indeterminate end moments. Mathematically the conditions may be expressed as:

(a) Total change in slope $= 0$

i.e., $$\int_0^l \frac{d^2y}{dx^2}\,dx = \frac{1}{E}\int_0^l \frac{\mu + M'}{I}\,dx = 0$$

where $\mu =$ bending moment at any section on an identical beam with simply-supported ends and identical loading

$M' =$ bending moment at that section due to the fixing couples at the ends

μ, M' and I are functions of x, the coordinate along the span. This condition is equivalent to saying that the areas under the $\frac{\mu}{I}$ and the $\frac{M'}{I}$ curves for the beam are equal.

Substituting the value of M'

$$M' = M_A + (M_B - M_A)\frac{x}{l}$$

where $M_A =$ moment at end A

$M_B =$ moment at end B

See Fig. 6.

We get

$$\int_0^l \frac{\mu}{I}\,dx + M_A \int_0^l \frac{dx}{I} + \frac{M_B - M_A}{l}\int_0^l \frac{x}{I}\,dx = 0 \qquad (1)$$

(b) The condition that the supports remain at the same level may be employed as follows:

$$\frac{d^2y}{dx^2} = \frac{\mu + M'}{EI}$$

Multiply both sides by X and integrate

$$\int_0^l x\,\frac{d^2y}{dx^2}\,dx = \int_0^l \frac{(\mu+M')}{EI}\,x\,dx$$

Integrating the left-hand side by parts

$$\int_0^l \frac{(\mu+M')x}{EI}.dx = \left[x\frac{dy}{dx} - y\right]_0^l = 0 \quad , \quad \text{since at } x = l,\ \frac{dy}{dx} = y = 0$$
$$\text{and} \quad " \quad X = 0, \quad " \quad "$$

$$\therefore \int_0^l \frac{\mu x}{I}\,dx + M_A\int_0^l \frac{x\,dx}{I} + \frac{M_B - M_A}{l}\int_0^l \frac{x^2}{I}\,dx = 0 \qquad (2)$$

Another way of stating this condition is that the centroids of the areas under the curves $\frac{\mu}{I}$ and $\frac{M'}{I}$ lie in the same vertical line. μ , the bending moment distribution with simply supported ends, is easily determined for a given loading so that equations (1) and (2) may be solved simultaneously to give M_A and M_B the end moments.

While this evaluation may be performed by algebraic manipulation, it was found more convenient and rapid (without any loss of exactness) to employ the moment-area principle, especially since the bending moment diagrams for the loading have triangular forms (or forms reducible to the sum of a rectangle and a triangle) and are peculiarly adapted to rapid calculation of areas. The influence curves for curvature, slope, and deflection are calculated for the beam under the action of each control and are shown in Figs. 20, 21, and 22.

REFERENCES

1. Galcit Transonic Research Group: "Problems in Shock Reflection". Galcit Final Report to A. A. F. under Contract No. W33-038ac-1717 (11592)

2. H. W. Liepmann and A. E. Puckett: Introduction to Aerodynamics of a Compressible Fluid. John Wiley and Sons. New York, N. Y. (1946).

3. I. Irving Pinkel: "Equations for the Design of Two-dimensional Supersonic Nozzles". N. A. C. A. R. M. No. E8B02. (June, 1948).

4. A. E. Puckett: "Supersonic Nozzle Design". Journal of Applied Mechanics. Vol. 13, No. 4. (December, 1946).

5. Kuno Foelsch: "A New Method of Designing Two-dimensional Laval Nozzles for a Parallel and Uniform Jet". North American Aviation Report No. NA-46-235. (1946).

6. A. E. Puckett: "Design and Operation of a 12" Supersonic Wind Tunnel". Presented at the annual summer meeting of the Institute of the Aeronautical Sciences. Los Angeles, California. (1948).

7. H. W. Liepmann and Harry Ashkenas: "Shock Wave Oscillations in Wind Tunnels". Galcit Progress Report to A. A. F. on Supplement No. 6 to Contract No. W33-038ac-1717(11592).

8. A. Kantrowitz and C. du P. Donaldson: "Supersonic Diffusers". N. A. C. A. Wartime Report L 713. (1945).

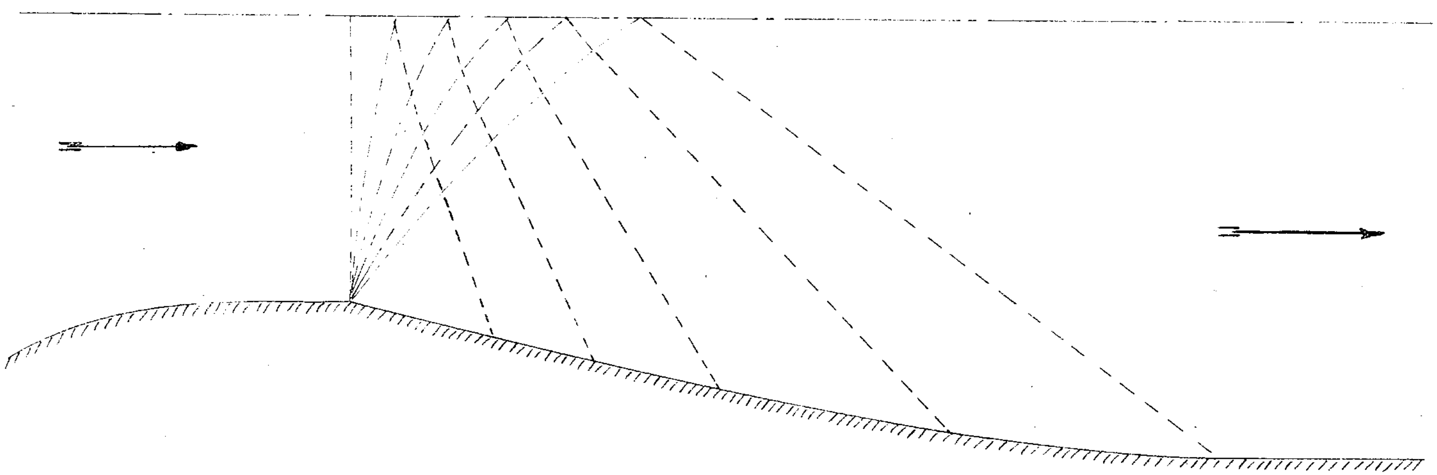

FIG. 1

SKETCH OF NOZZLE

USING CORNER AT THROAT

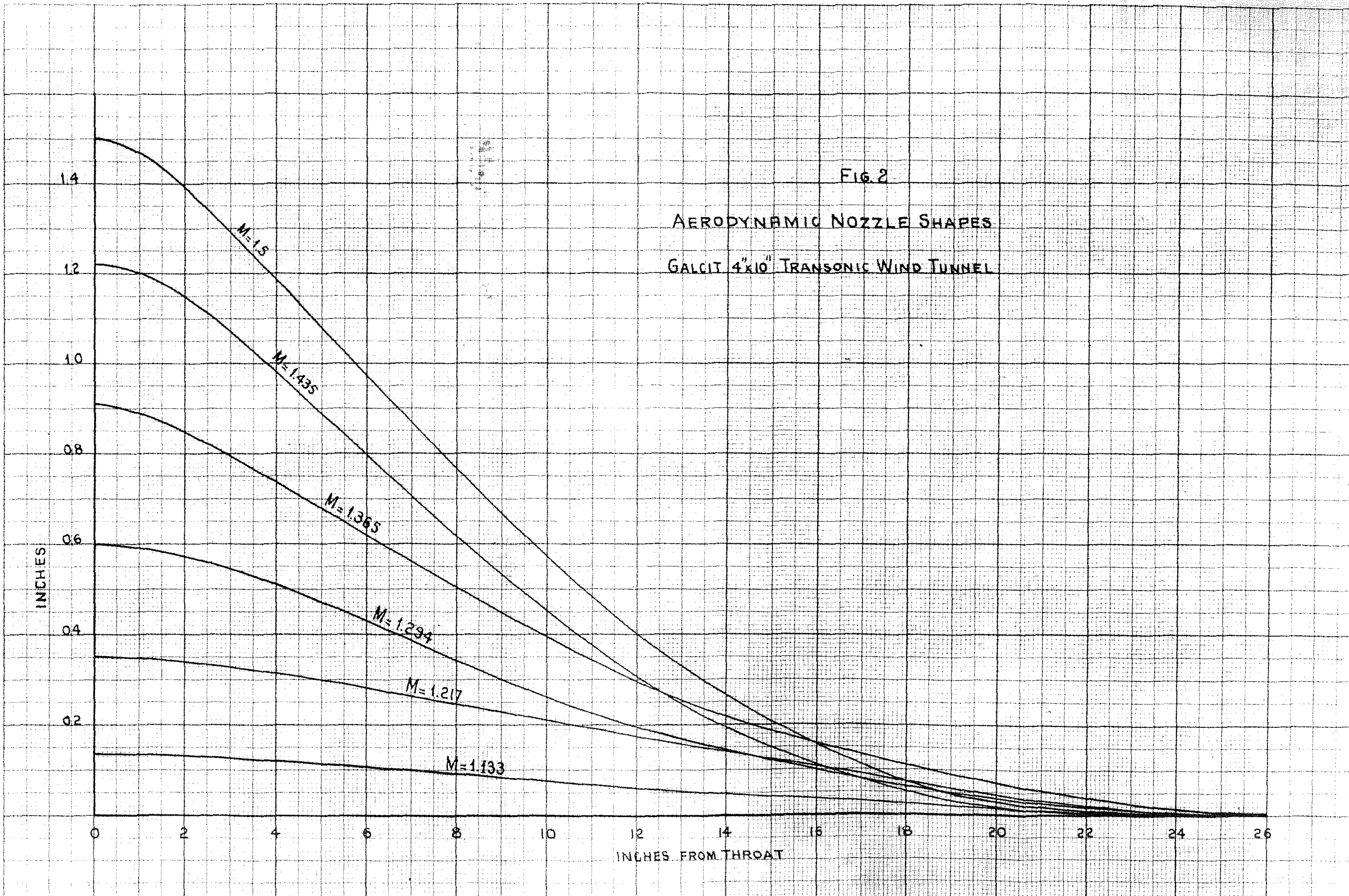

FIG. 2

AERODYNAMIC NOZZLE SHAPES

GALCIT 4"x10" TRANSONIC WIND TUNNEL

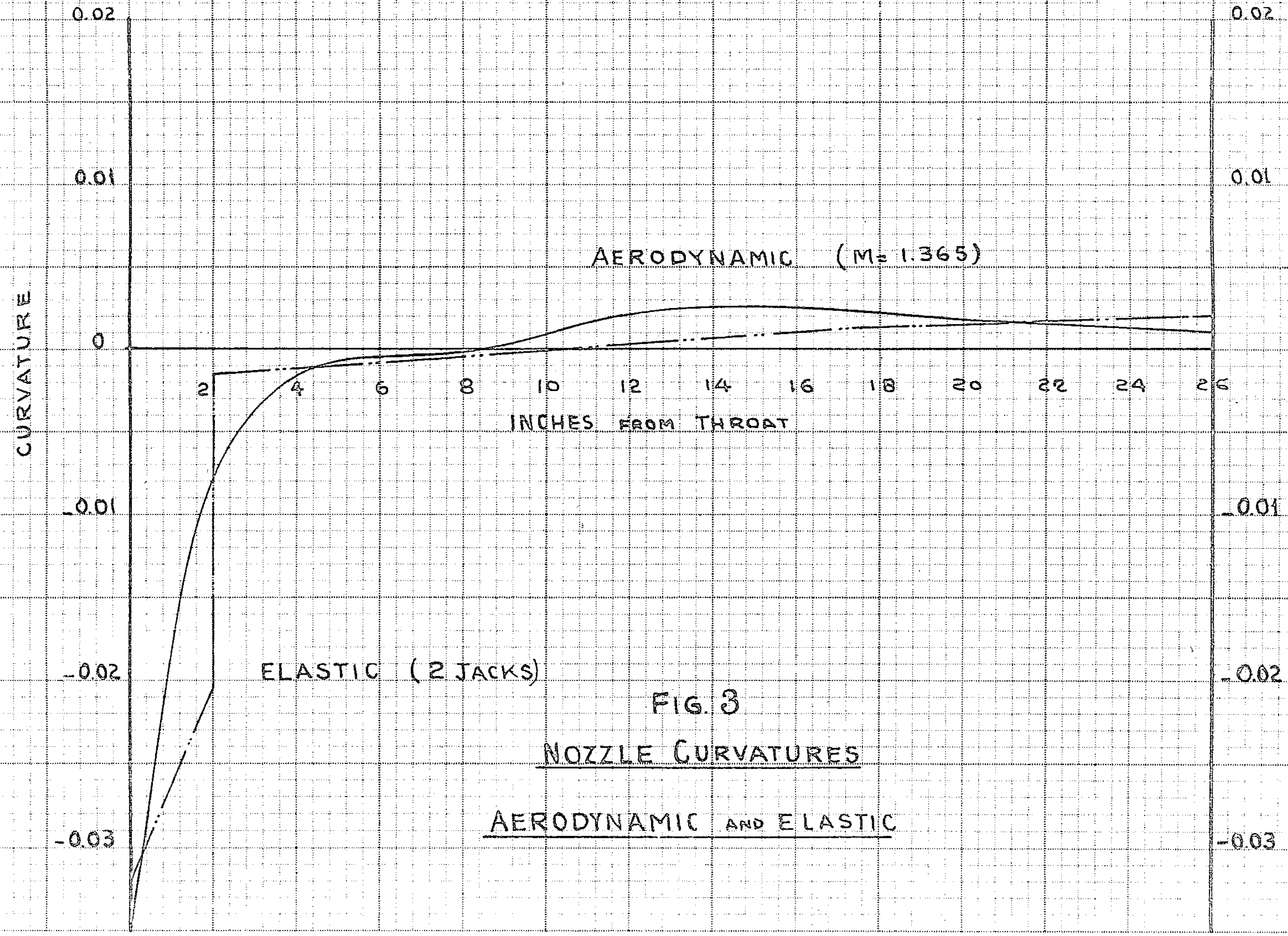

FIG. 3

NOZZLE CURVATURES

AERODYNAMIC AND ELASTIC

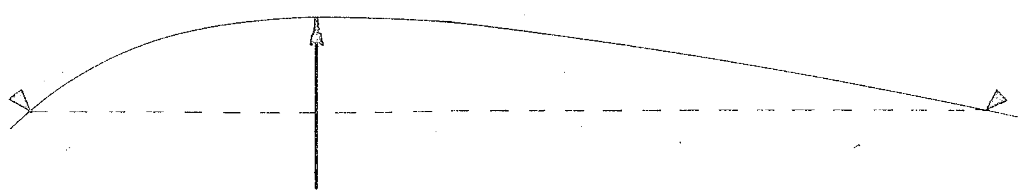

Fig. 4

Elastic Shape of Beam with Simply Supported Ends

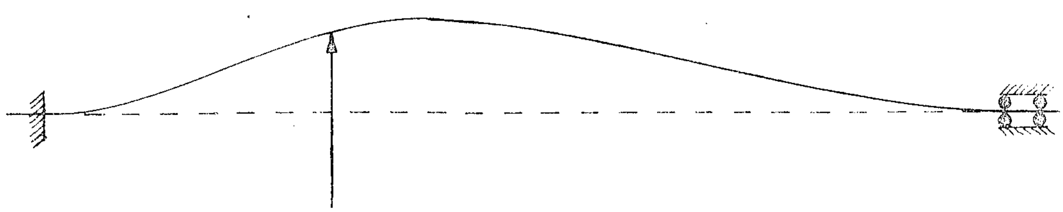

Fig. 5

Elastic Shape of Beam with Direction Fixed Ends

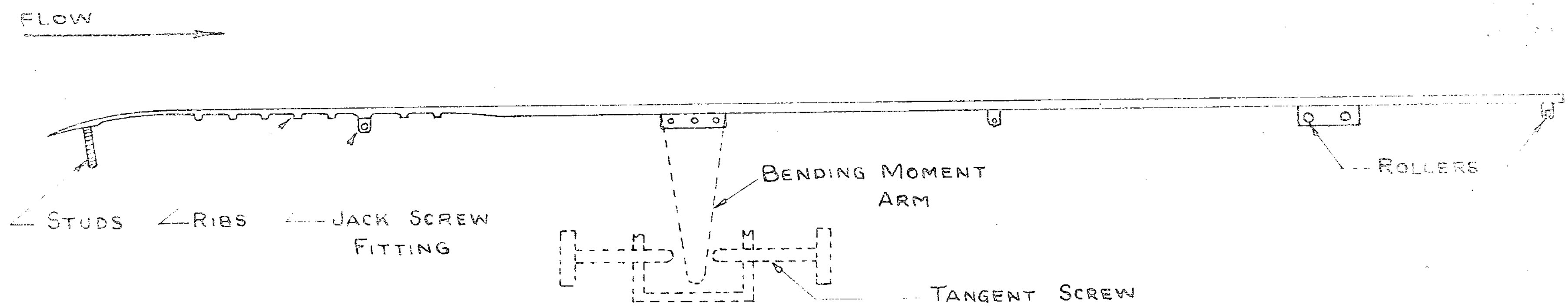

NOZZLE PLATE & FITTINGS

FIG. 6

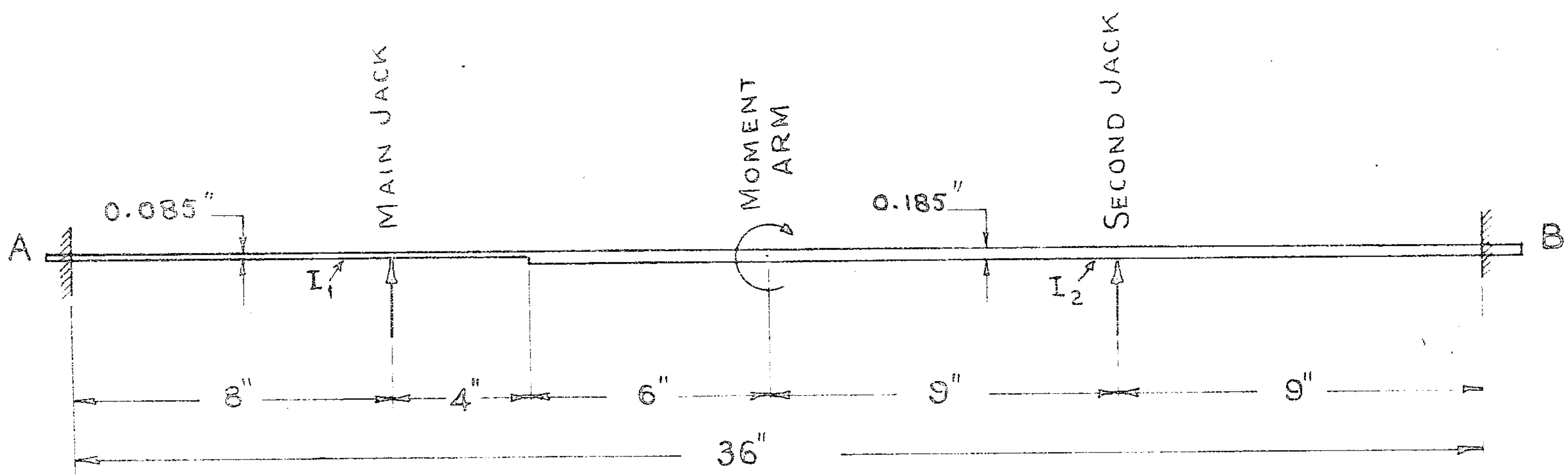

REPRESENTATION AS FIXED-END BEAM

Fig. 7

Matching of Aerodynamic & Elastic Shapes
By Method of "Least Squares"
(M=1.365)

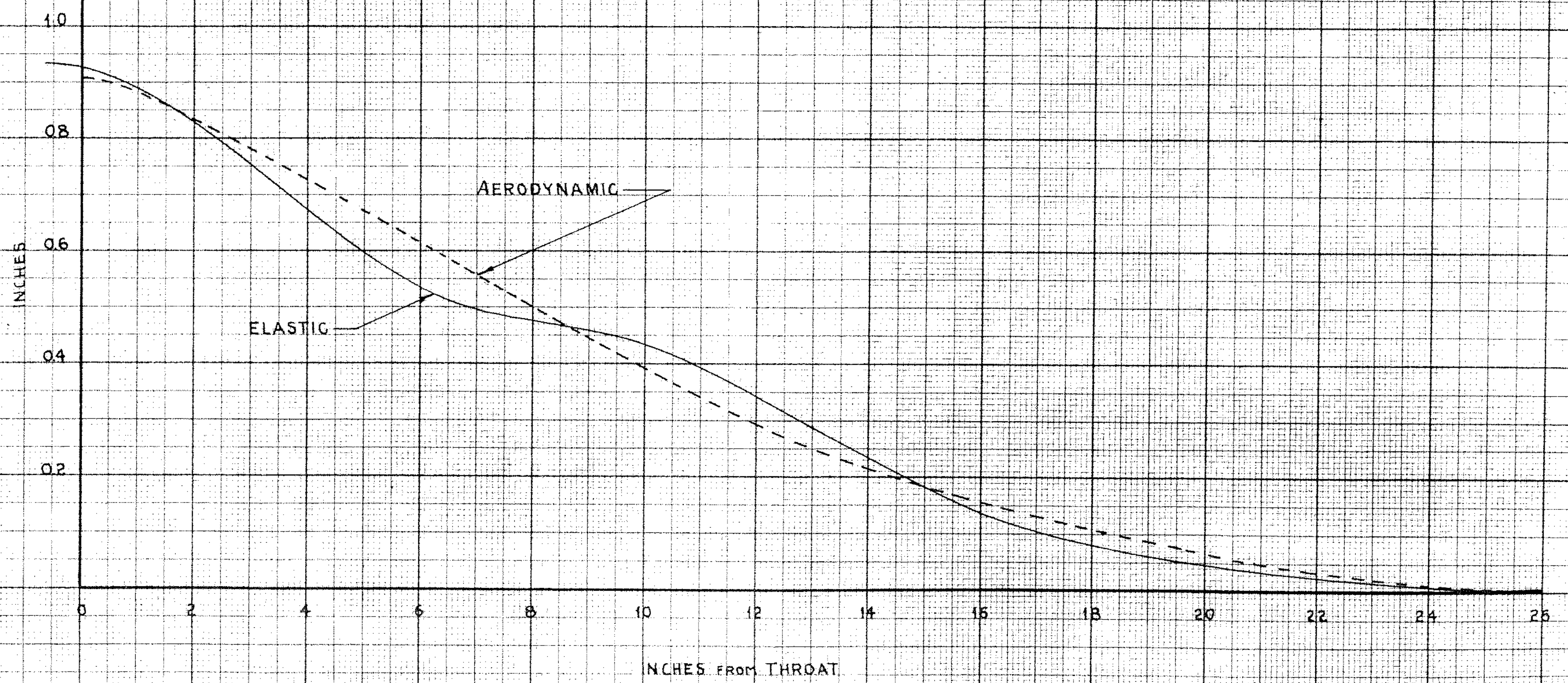

Fig. 8
Matching of the Aerodynamic & Elastic Shapes
(M=1.5)

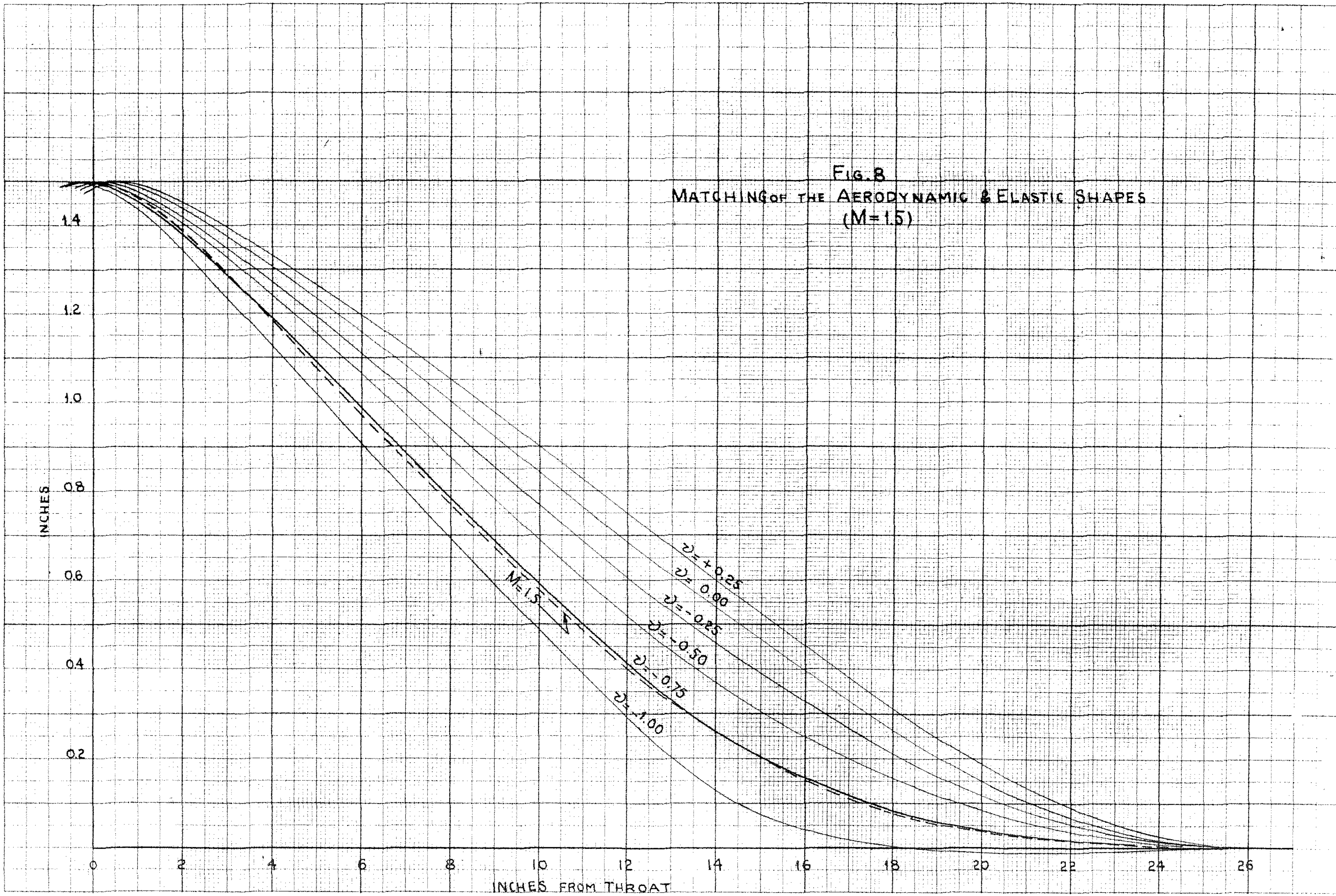

Fig. 9

MATCHED AERODYNAMIC AND ELASTIC SHAPES

M=1.435

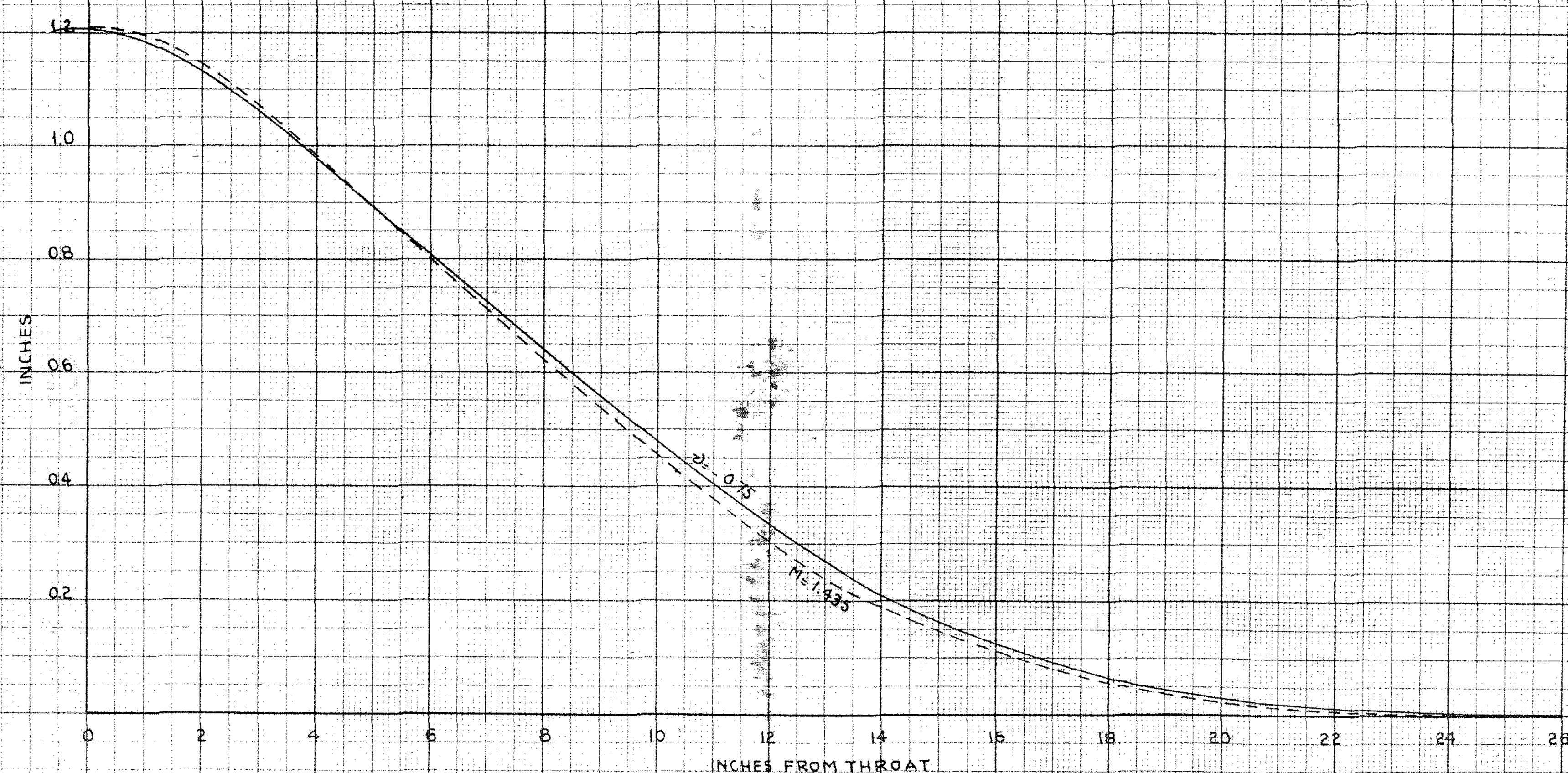

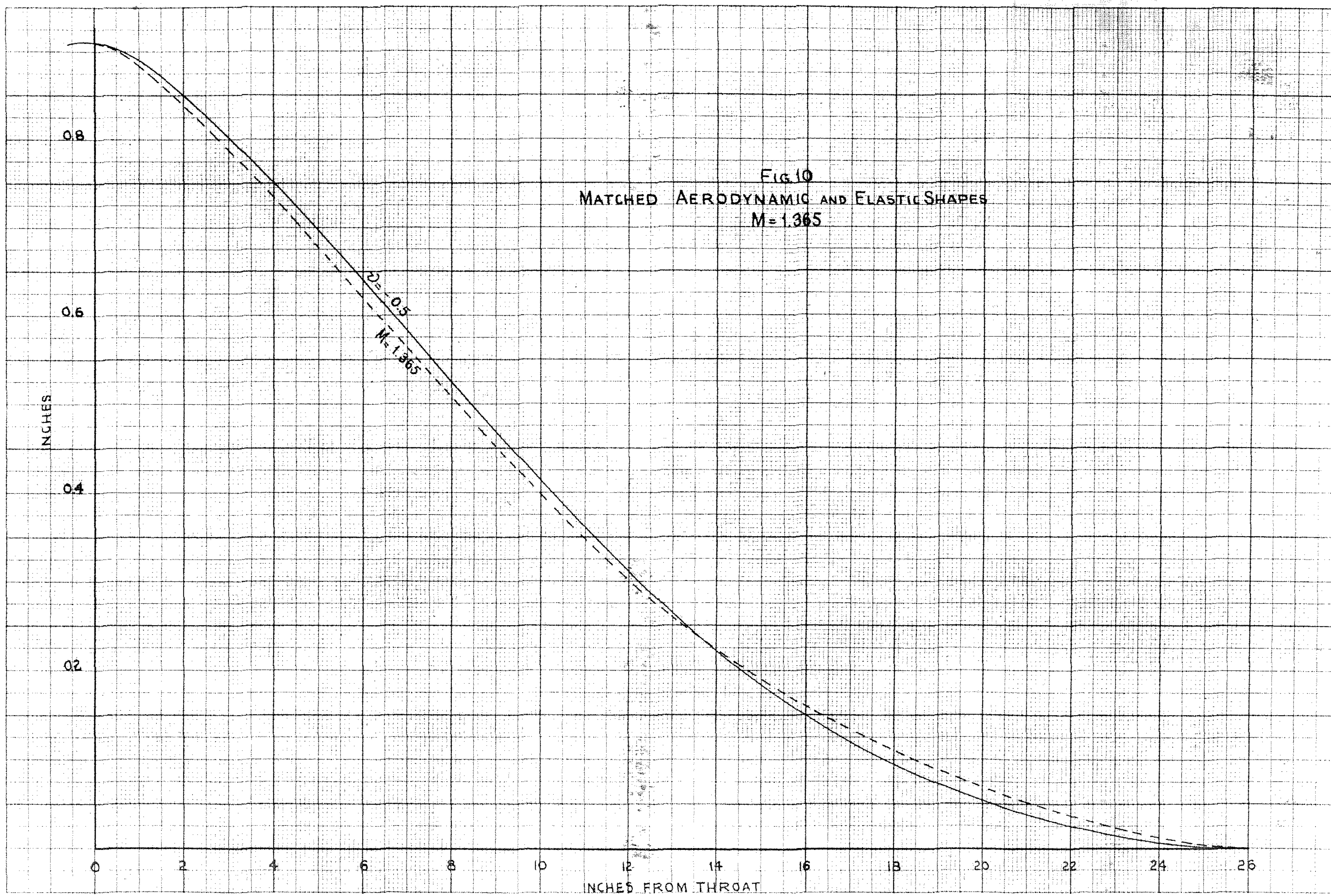

FIG. 10
MATCHED AERODYNAMIC AND ELASTIC SHAPES
M = 1.365

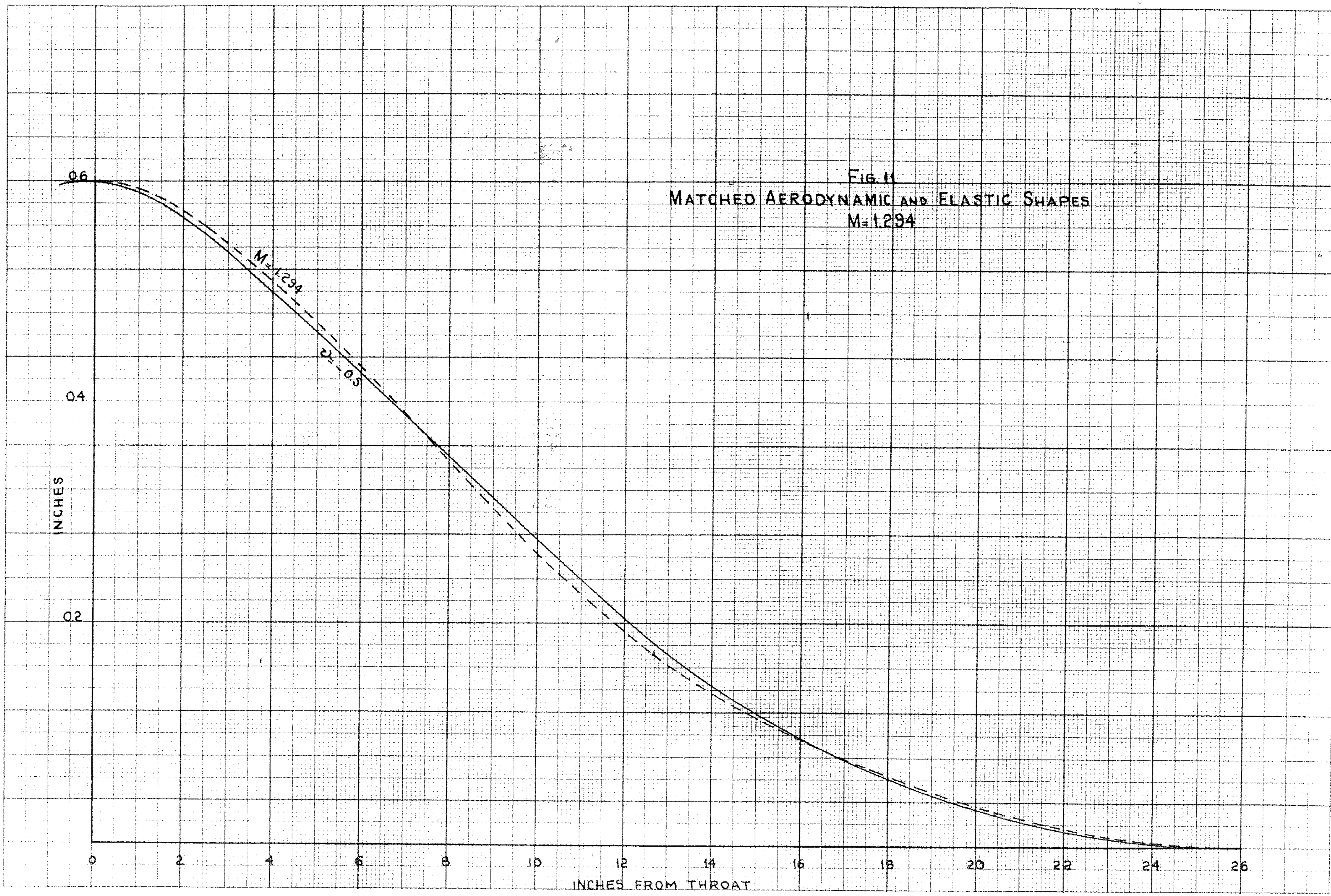

FIG. 11
MATCHED AERODYNAMIC AND ELASTIC SHAPES
M=1.294

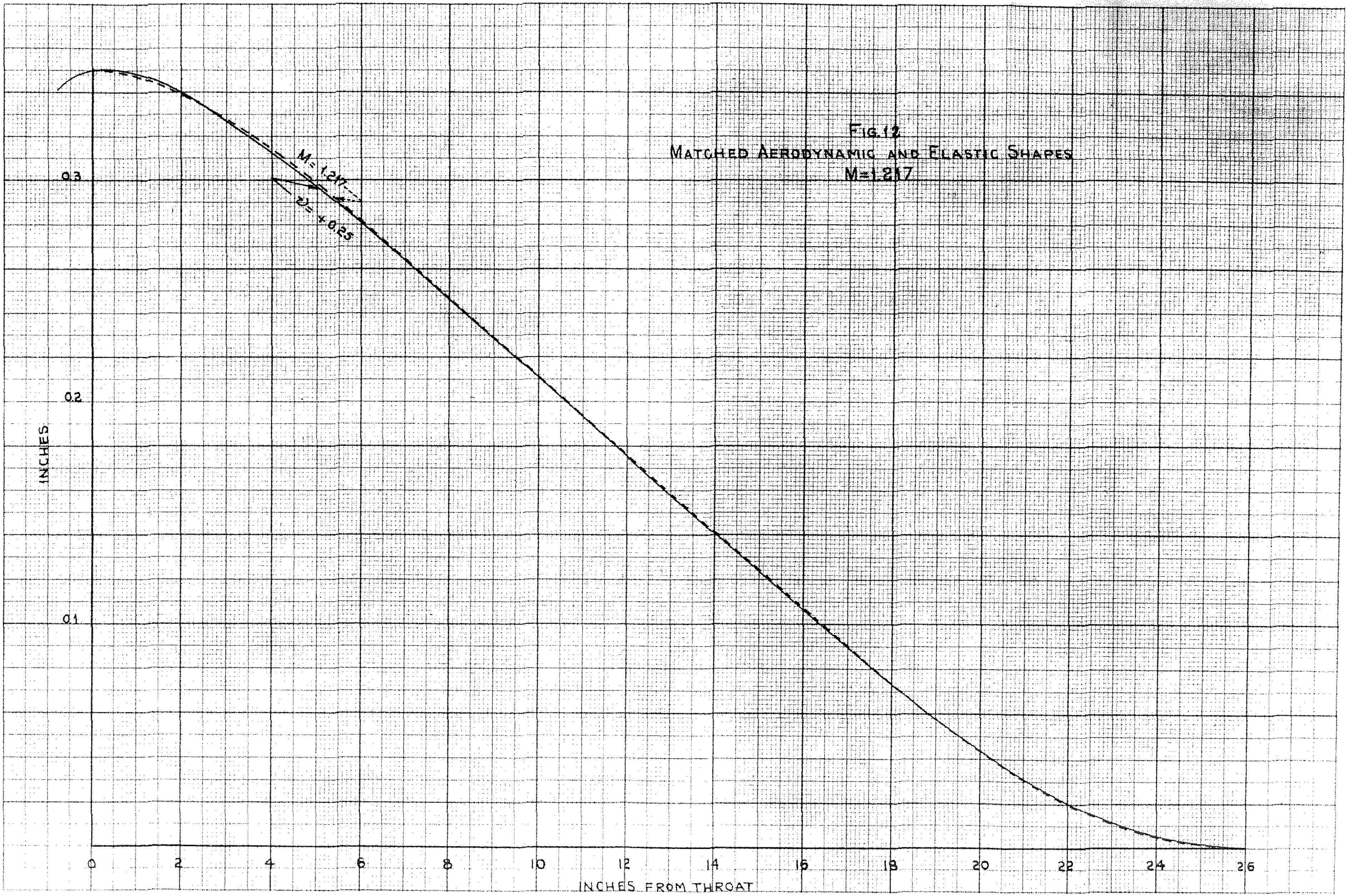

FIG. 12
MATCHED AERODYNAMIC AND ELASTIC SHAPES
M=1.217

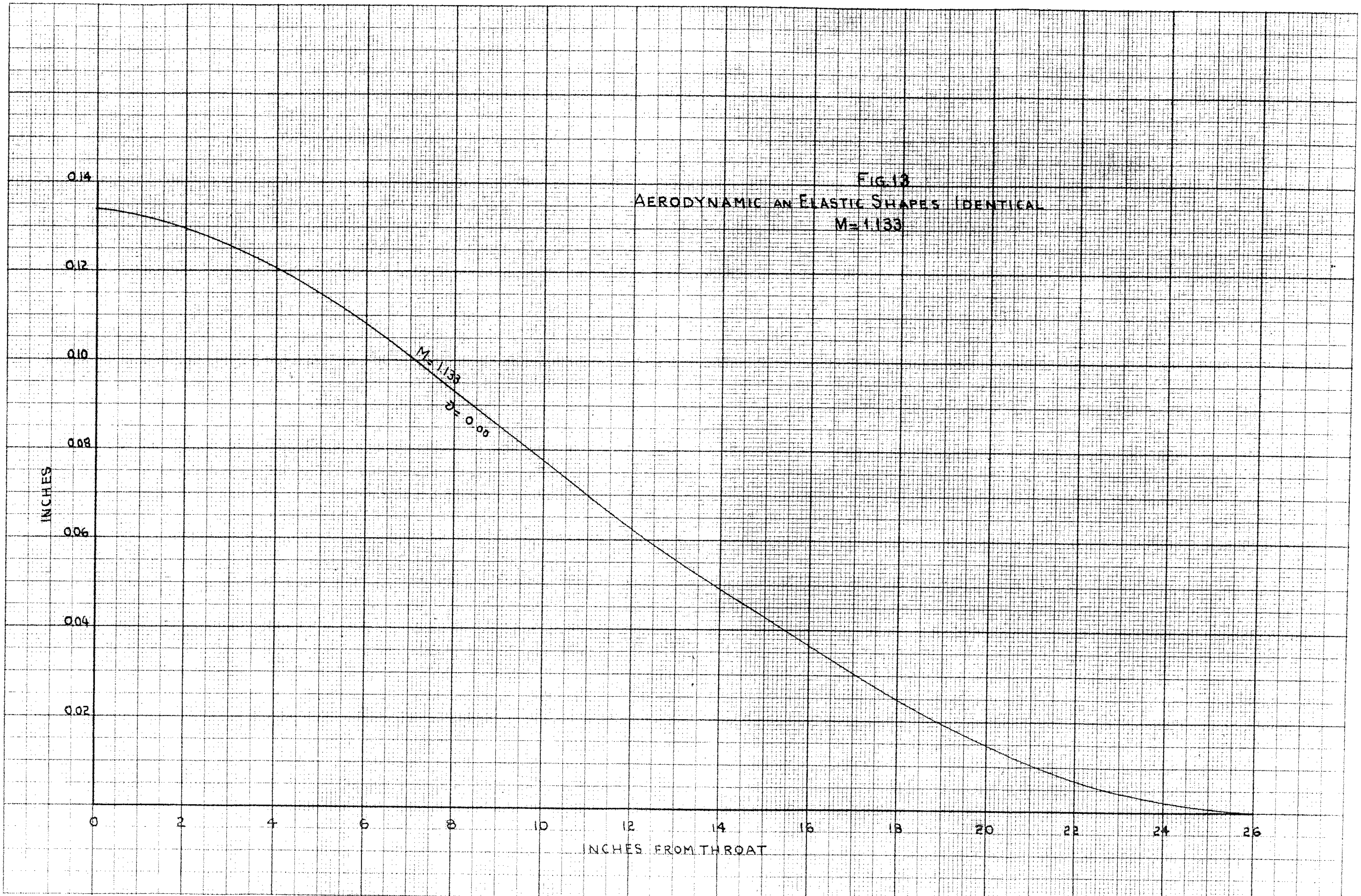

FIG. 13
AERODYNAMIC AN ELASTIC SHAPES IDENTICAL
M=1.133

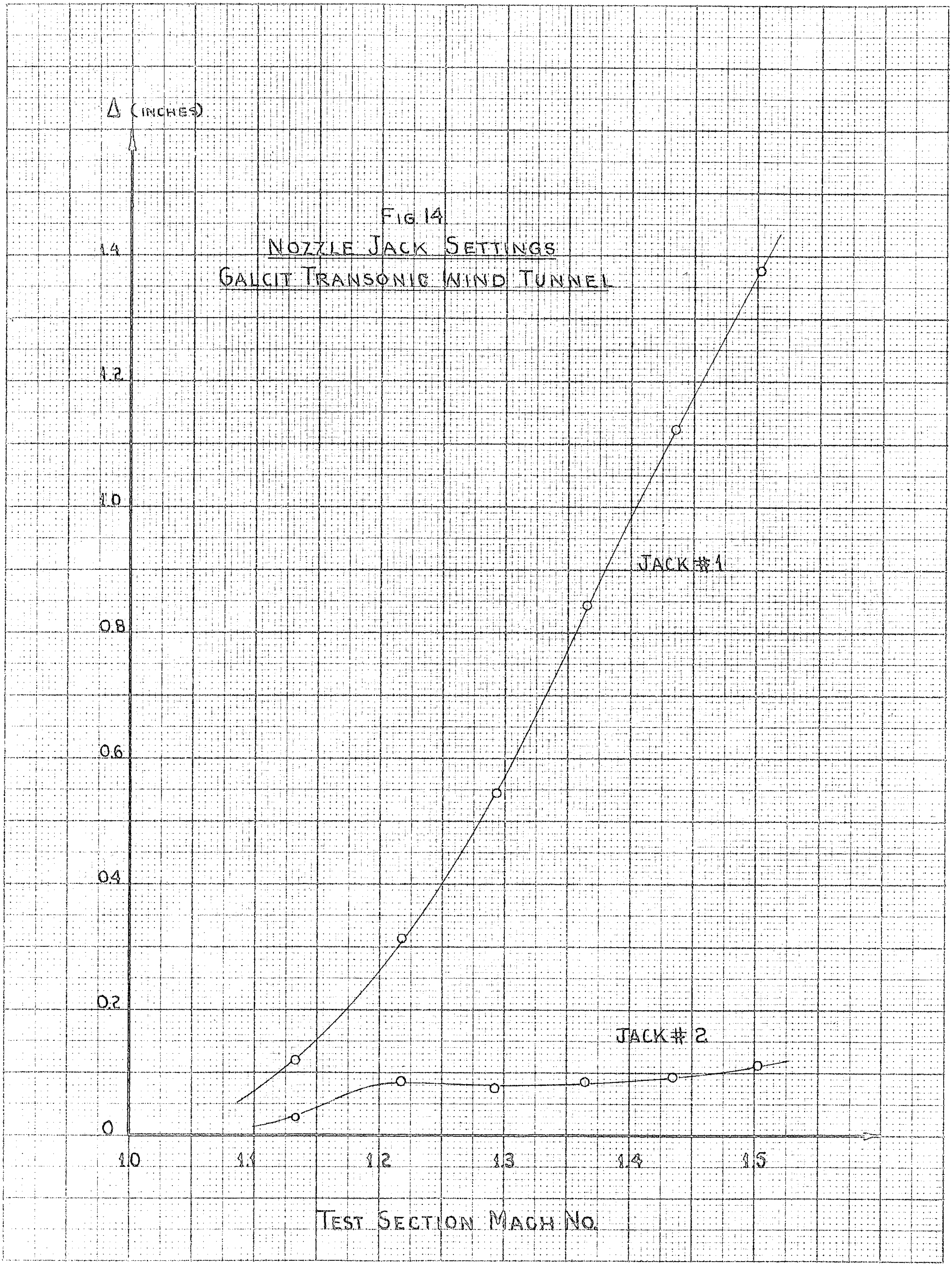

Δ (INCHES)
FIG 14
NOZZLE JACK SETTINGS
GALCIT TRANSONIC WIND TUNNEL
1.4
1.2
1.0
0.8
0.6
0.4
0.2
0
JACK #1
JACK # 2
1.0
1.1
1.2
1.3
1.4
1.5
TEST SECTION MACH NO.

TABLE I

CONTROL SETTINGS FOR THE GALCIT 4"x10" TRANSONIC TUNNEL

M	Δ" FOR JACK #1	Δ" FOR JACK #2
1.133	0.120	0.029
1.217	0.311	0.088
1.294	0.547	0.078
1.365	0.843	0.089
1.435	1.121	0.091
1.504	1.379	0.112

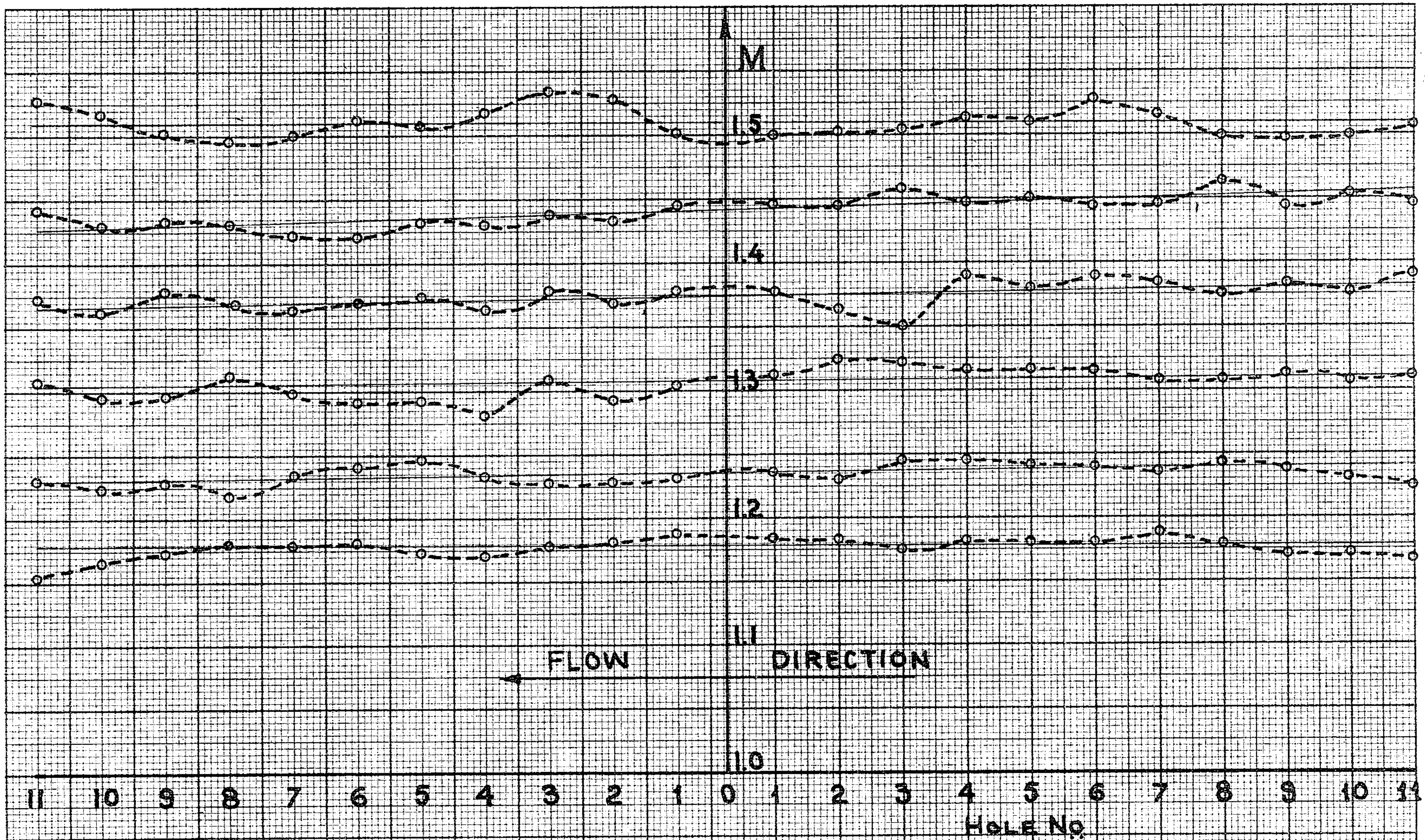

FIG. 15

HORIZONTAL
MACH NUMBER DISTRIBUTIONS
EMPTY TUNNEL

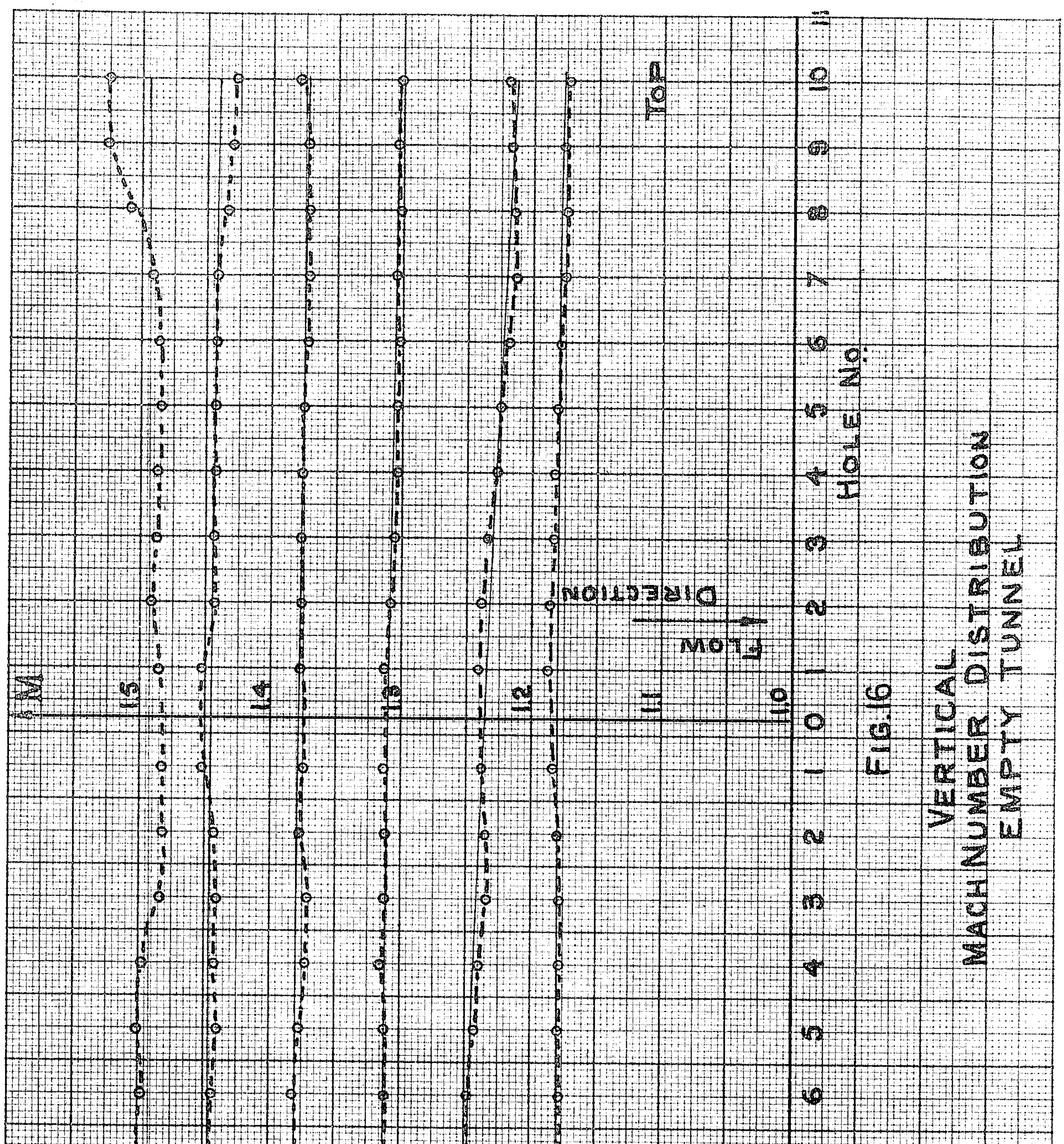

FIG.16

VERTICAL
MACH NUMBER DISTRIBUTION
EMPTY TUNNEL

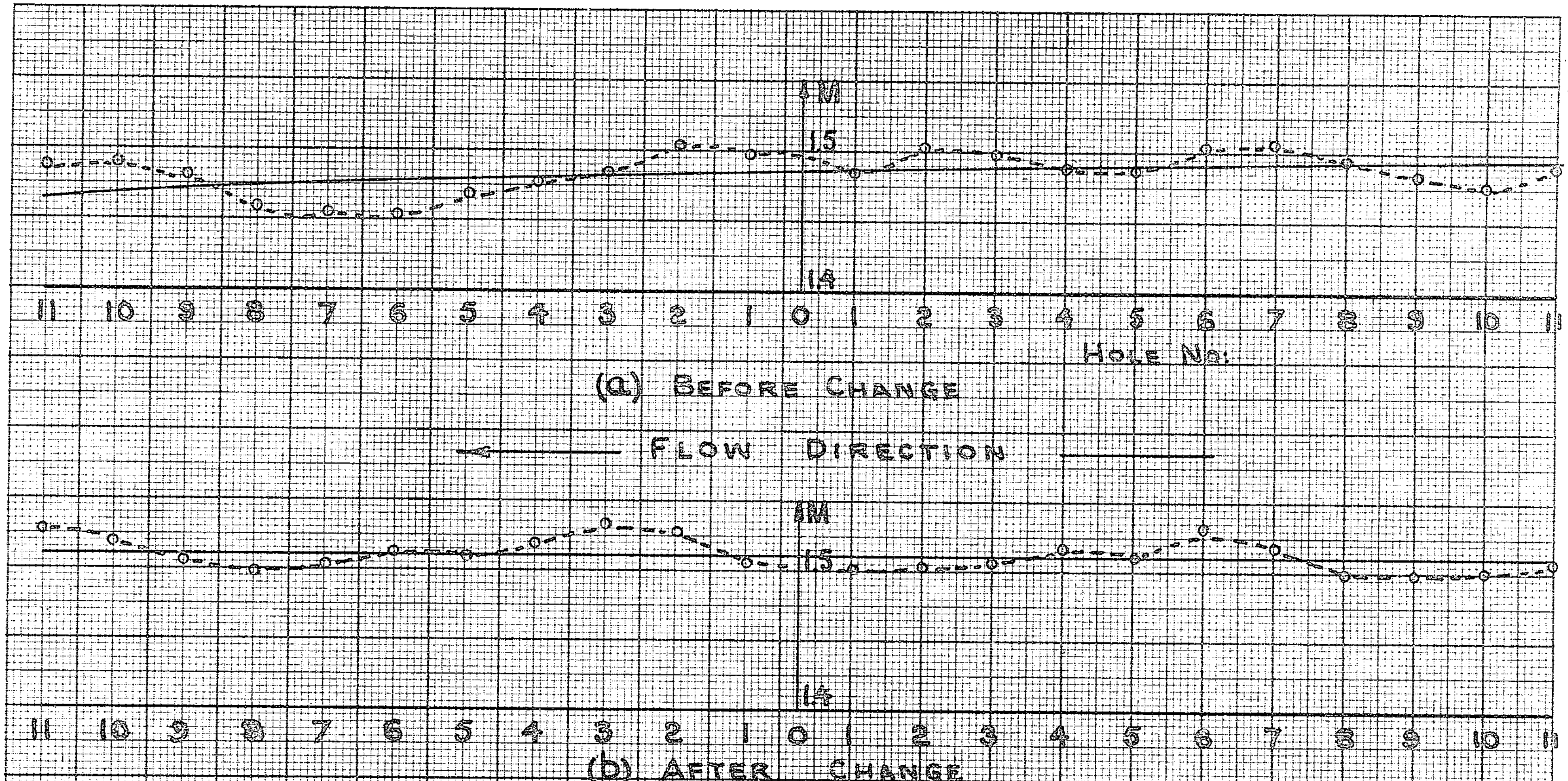

FIGS. 17 (a) & (b)

EFFECT OF CHANGE IN BOUNDARY LAYER CORRECTION
ON
HORIZONTAL MACH NUMBER DISTRIBUTION M = 1.5

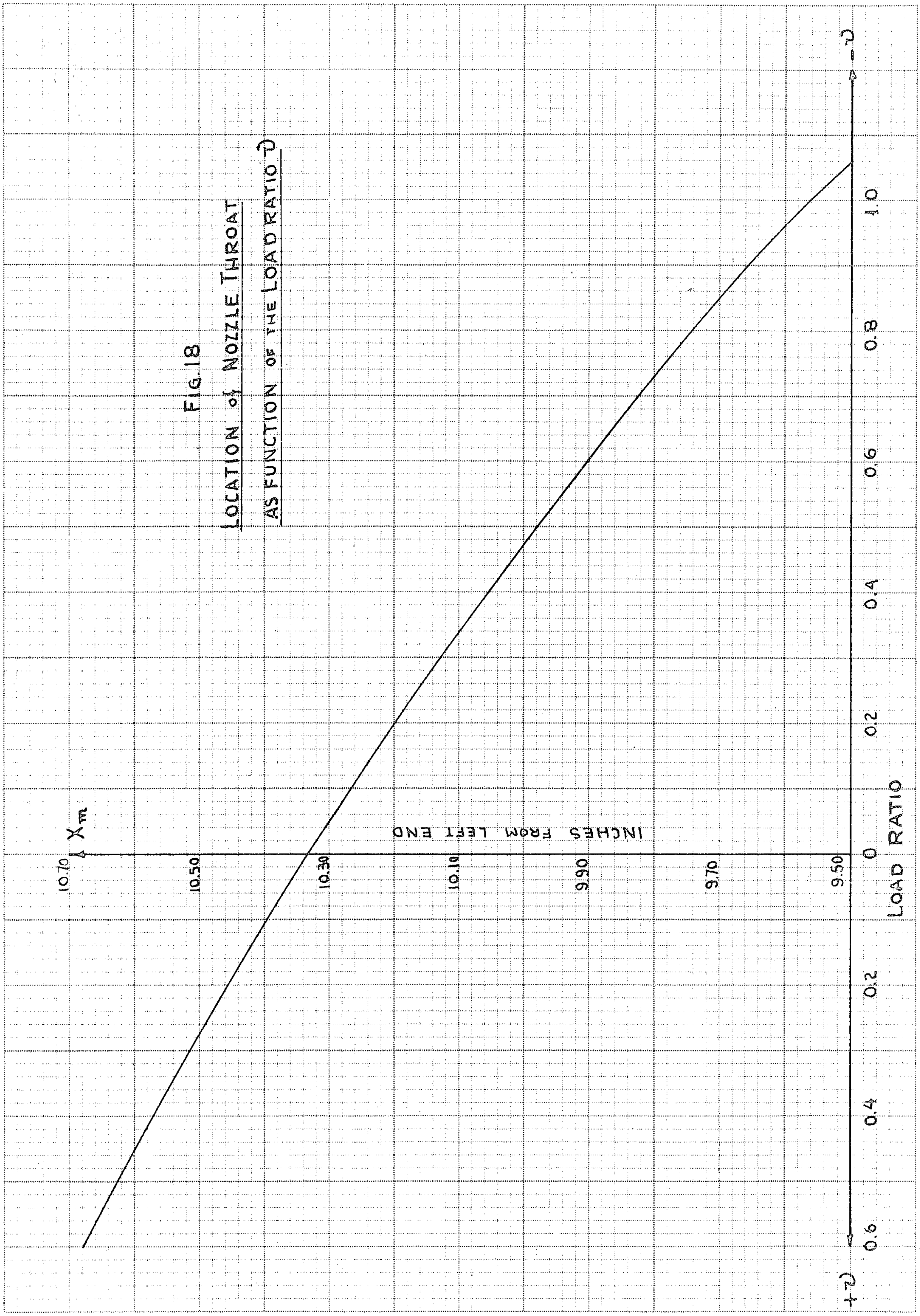

FIG. 18

LOCATION OF NOZZLE THROAT

AS FUNCTION OF THE LOAD RATIO ν

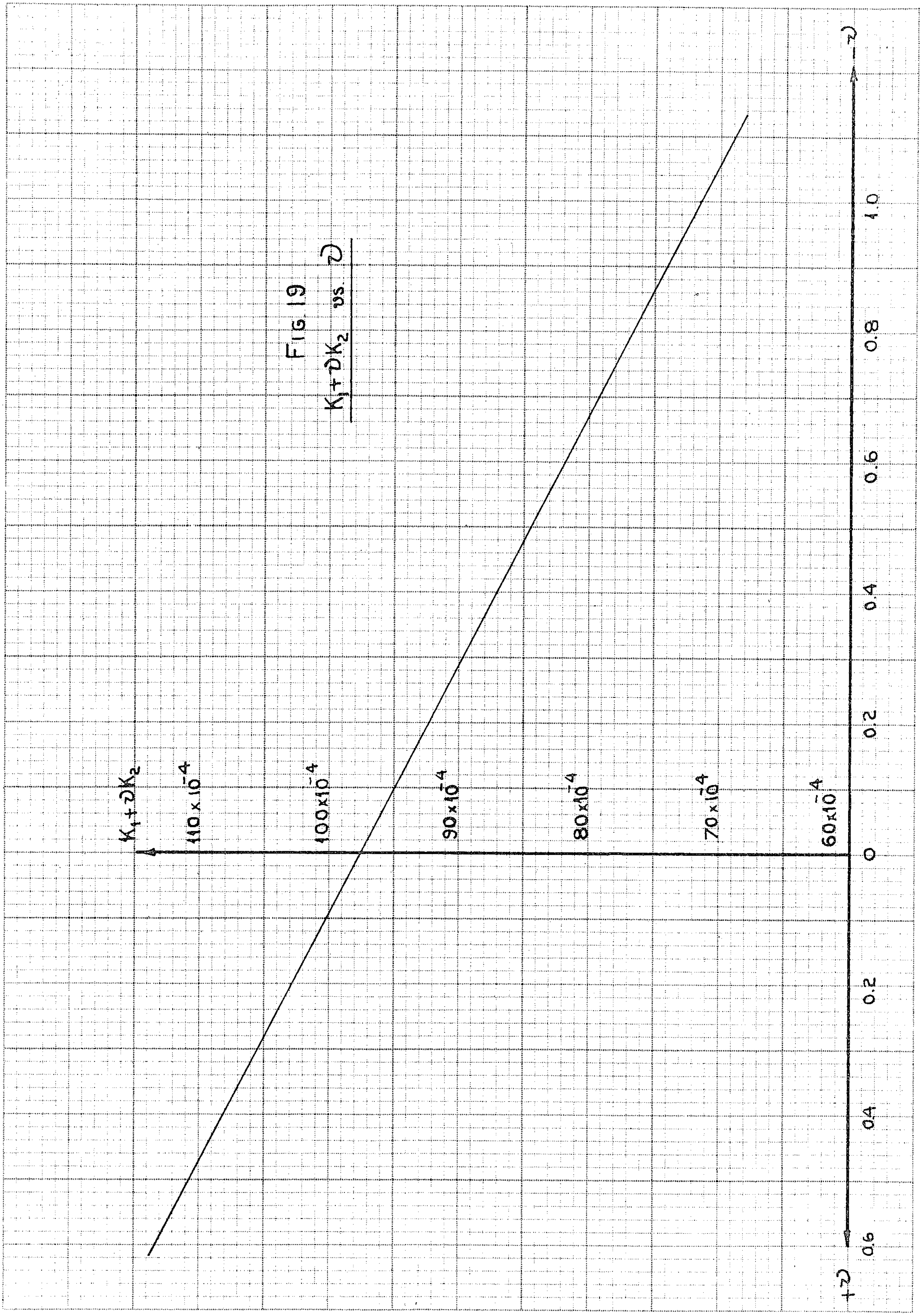
FIG 19
$K_1 + \nu K_2$ vs. ν
$K_1 + \nu K_2$
110×10^{-4}
100×10^{-4}
90×10^{-4}
80×10^{-4}
70×10^{-4}
60×10^{-4}
$-\nu$
1.0
0.8
0.6
0.4
0.2
0
0.2
0.4
0.6
$+\nu$

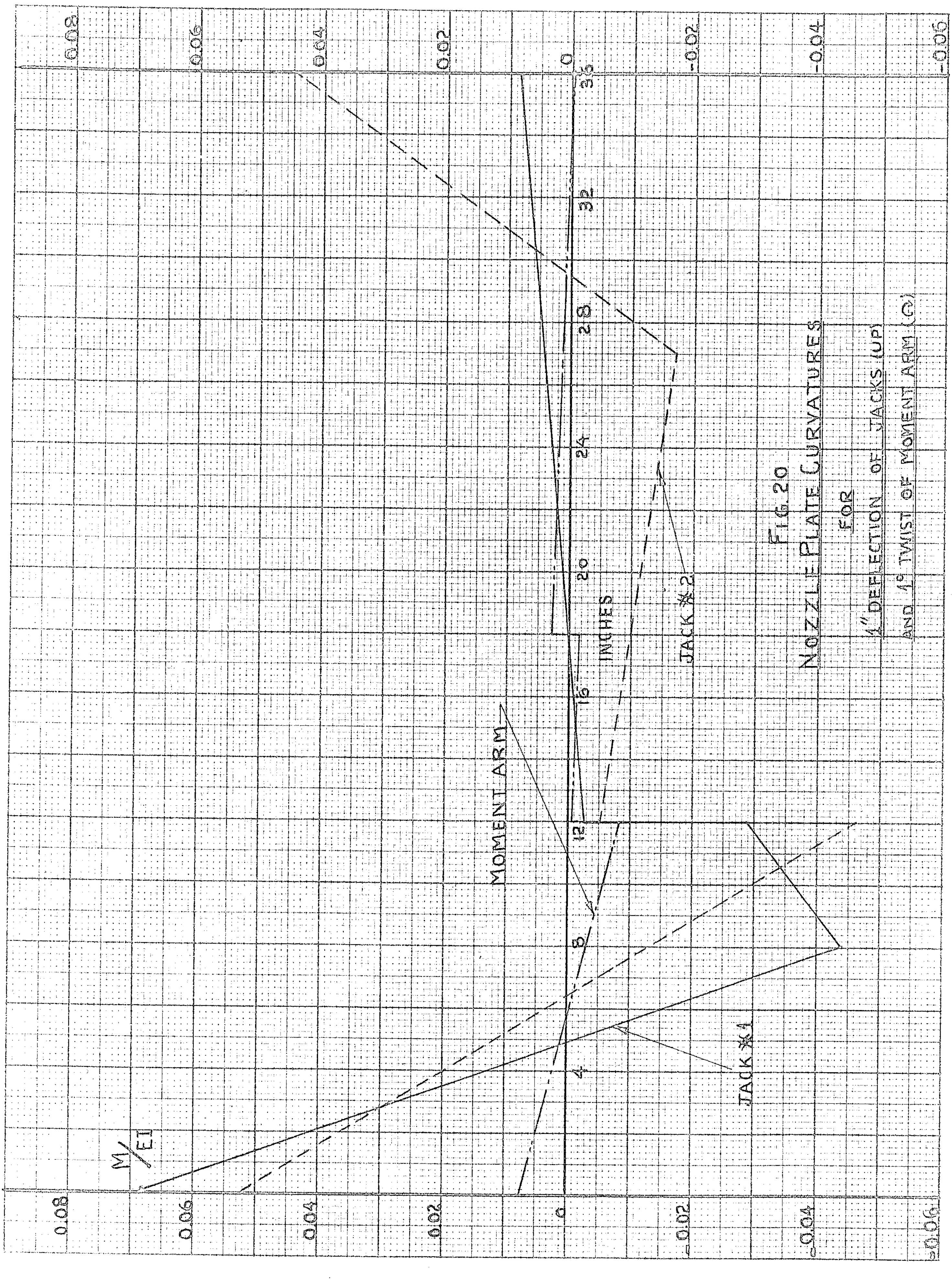

FIG. 20
NOZZLE PLATE CURVATURES
FOR
1" DEFLECTION OF JACKS (UP)
AND 4° TWIST OF MOMENT ARM (C)

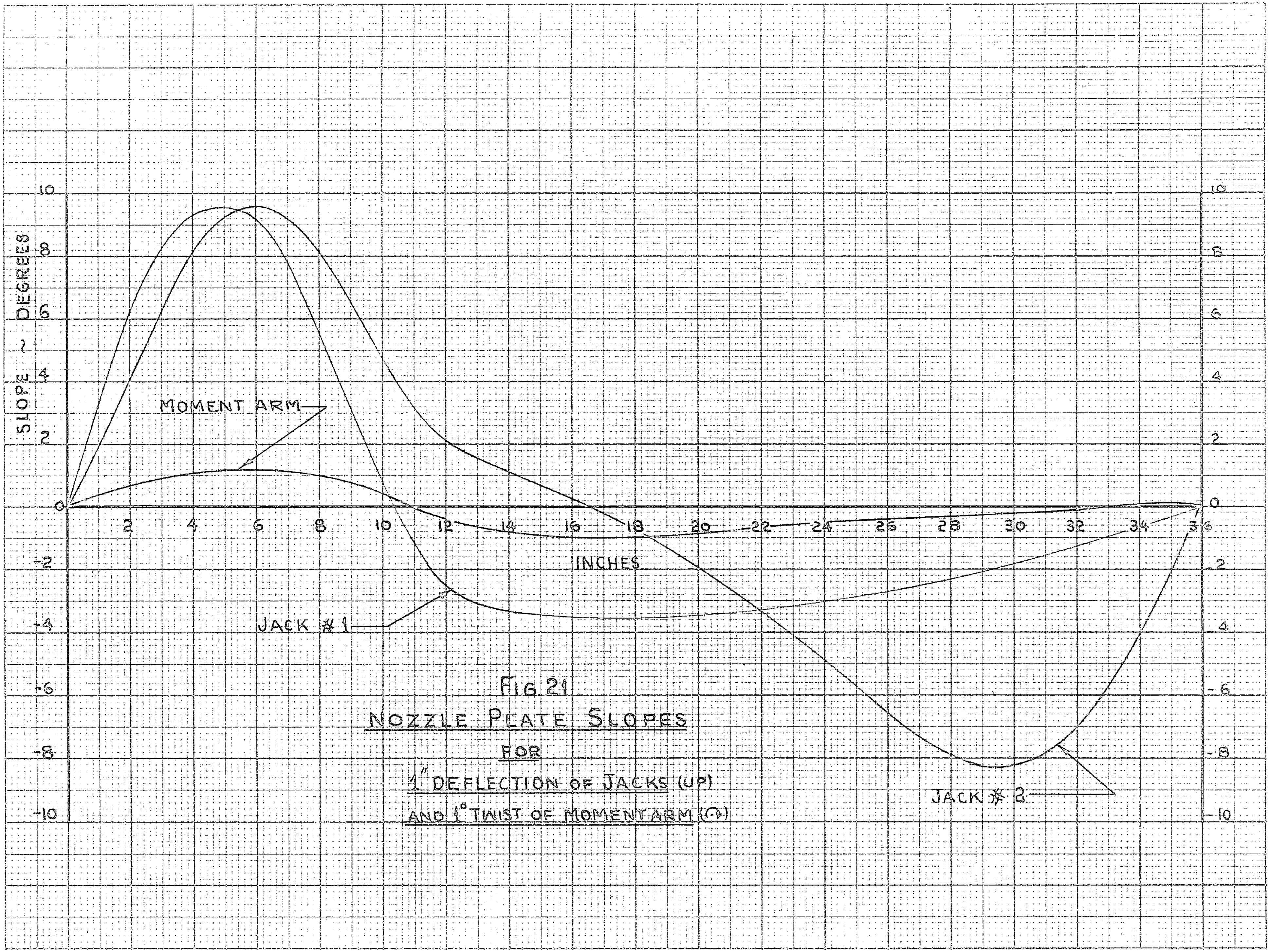

FIG. 21
NOZZLE PLATE SLOPES
FOR
1" DEFLECTION OF JACKS (UP)
AND 1° TWIST OF MOMENTARM (↻)

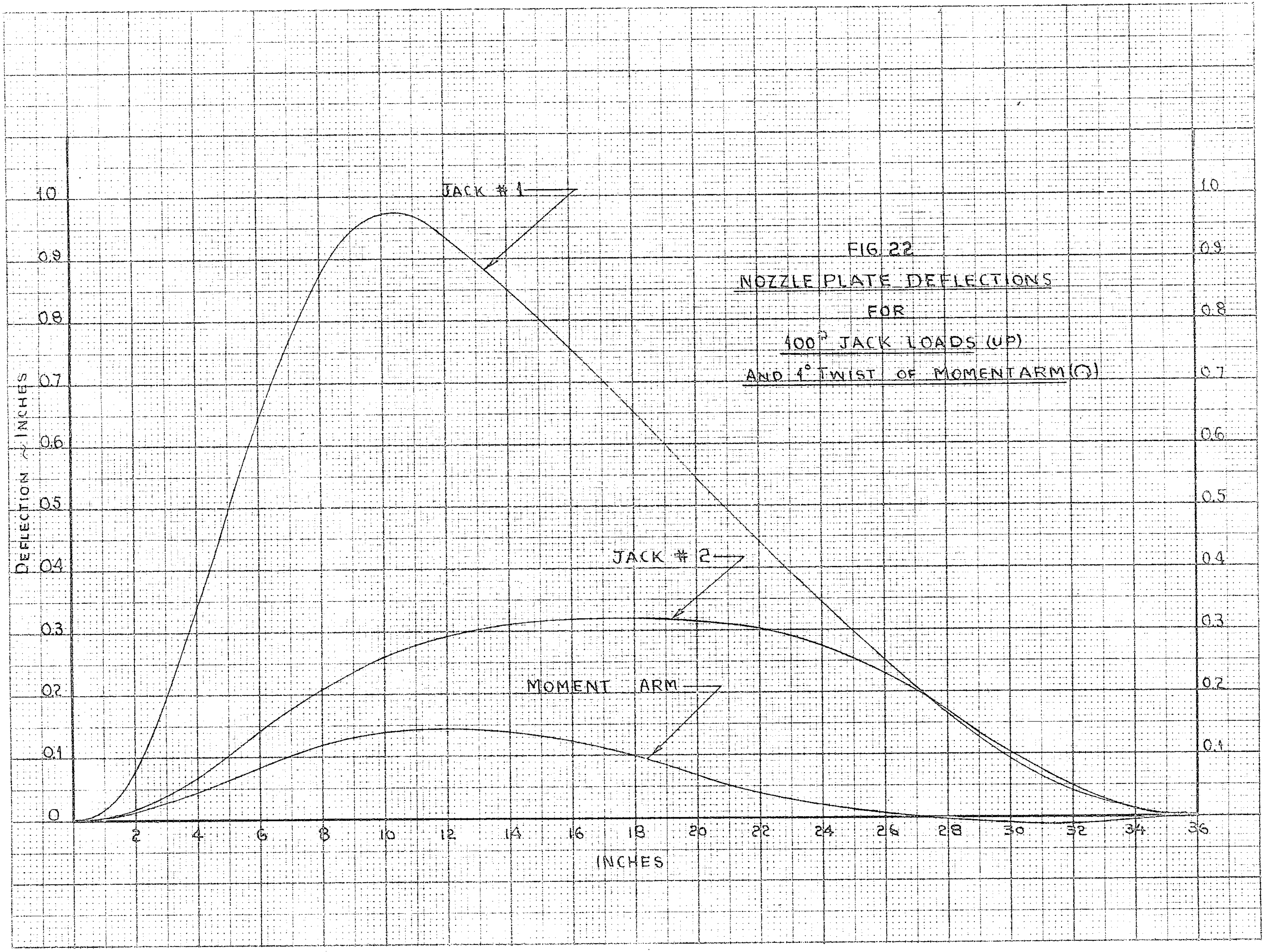
FIG 22
NOZZLE PLATE DEFLECTIONS
FOR
400# JACK LOADS (UP)
AND 4° TWIST OF MOMENT ARM
JACK # 1
JACK # 2
MOMENT ARM
DEFLECTION ~ INCHES
INCHES
0
0.1
0.2
0.3
0.4
0.5
0.6
0.7
0.8
0.9
1.0
2
4
6
8
10
12
14
16
18
20
22
24
26
28
30
32
34
36

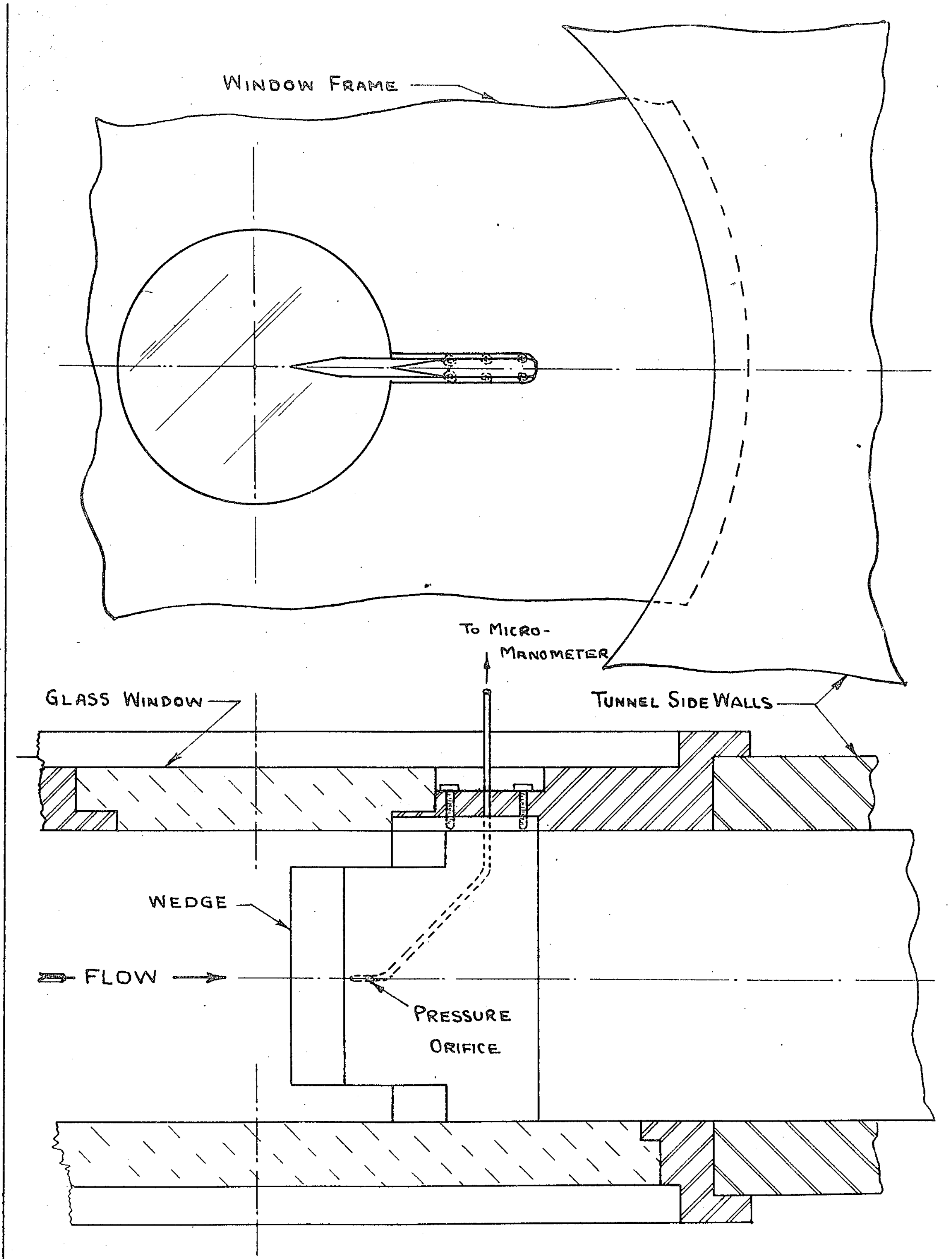

Fig. 23

Sketch showing Wedge installation in Tunnel

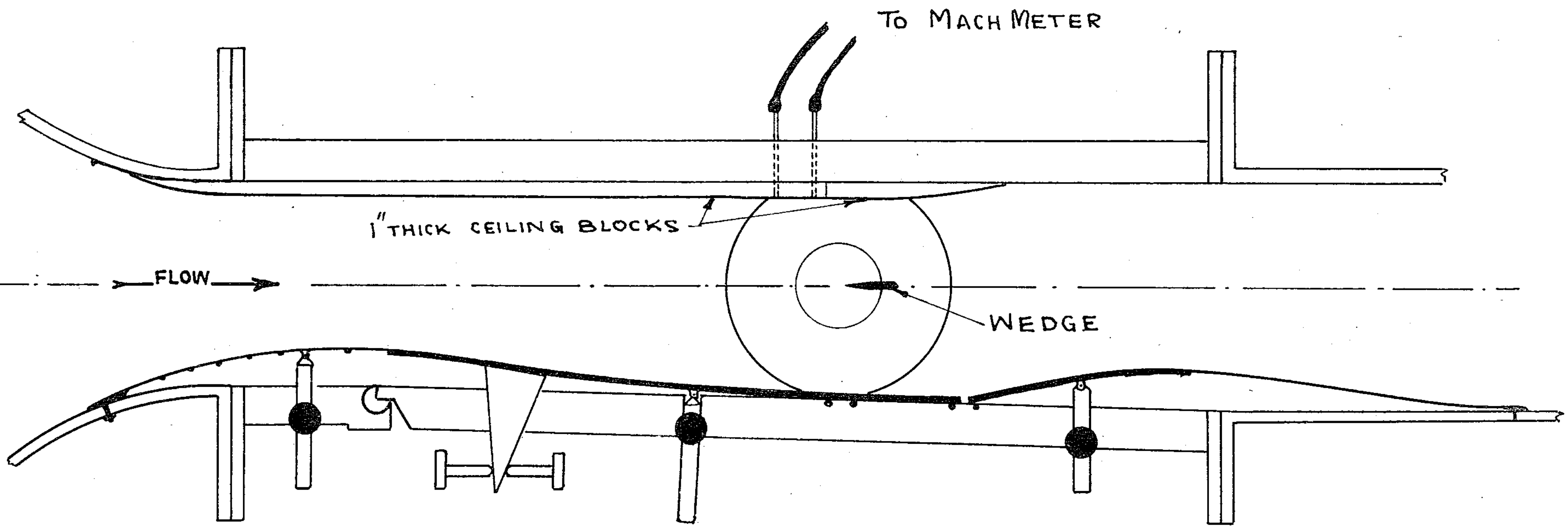

Fig: 24

Sketch of GALCIT 4"x10" Transonic Tunnel Test Section showing Flexible Nozzle, Wedge and Ceiling Blocks

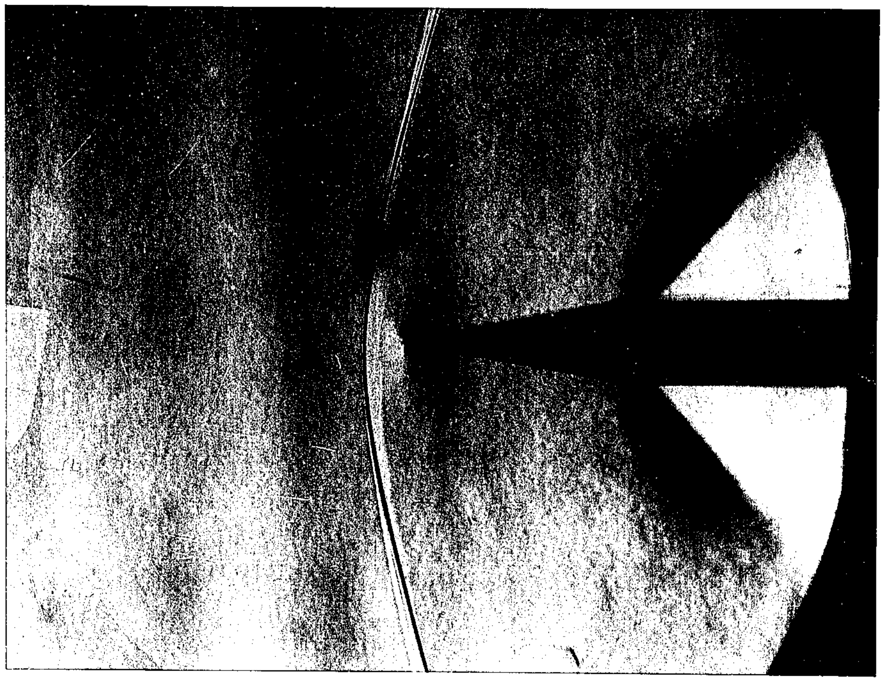

FIG: 25

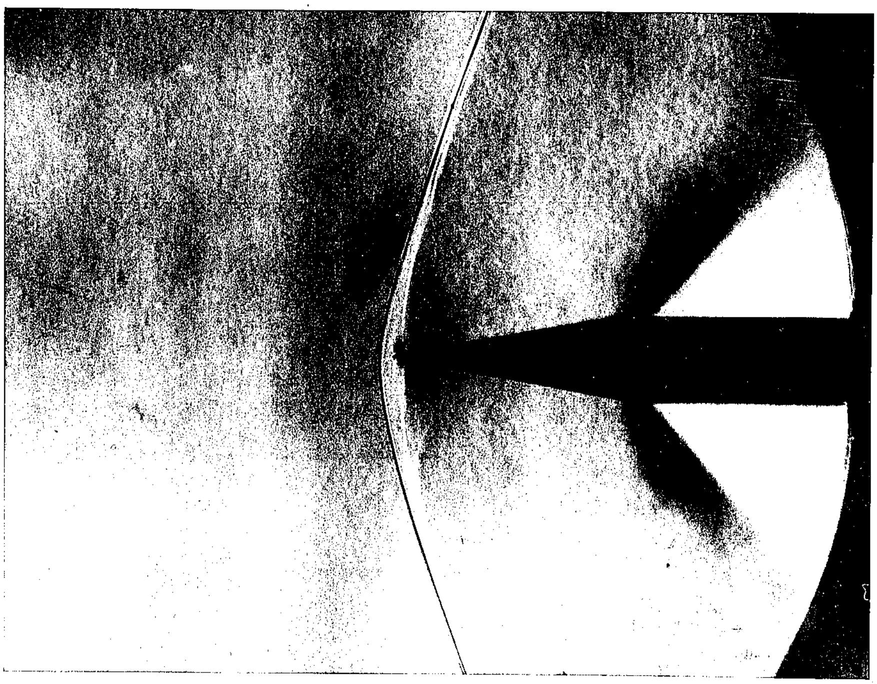

FIG: 26

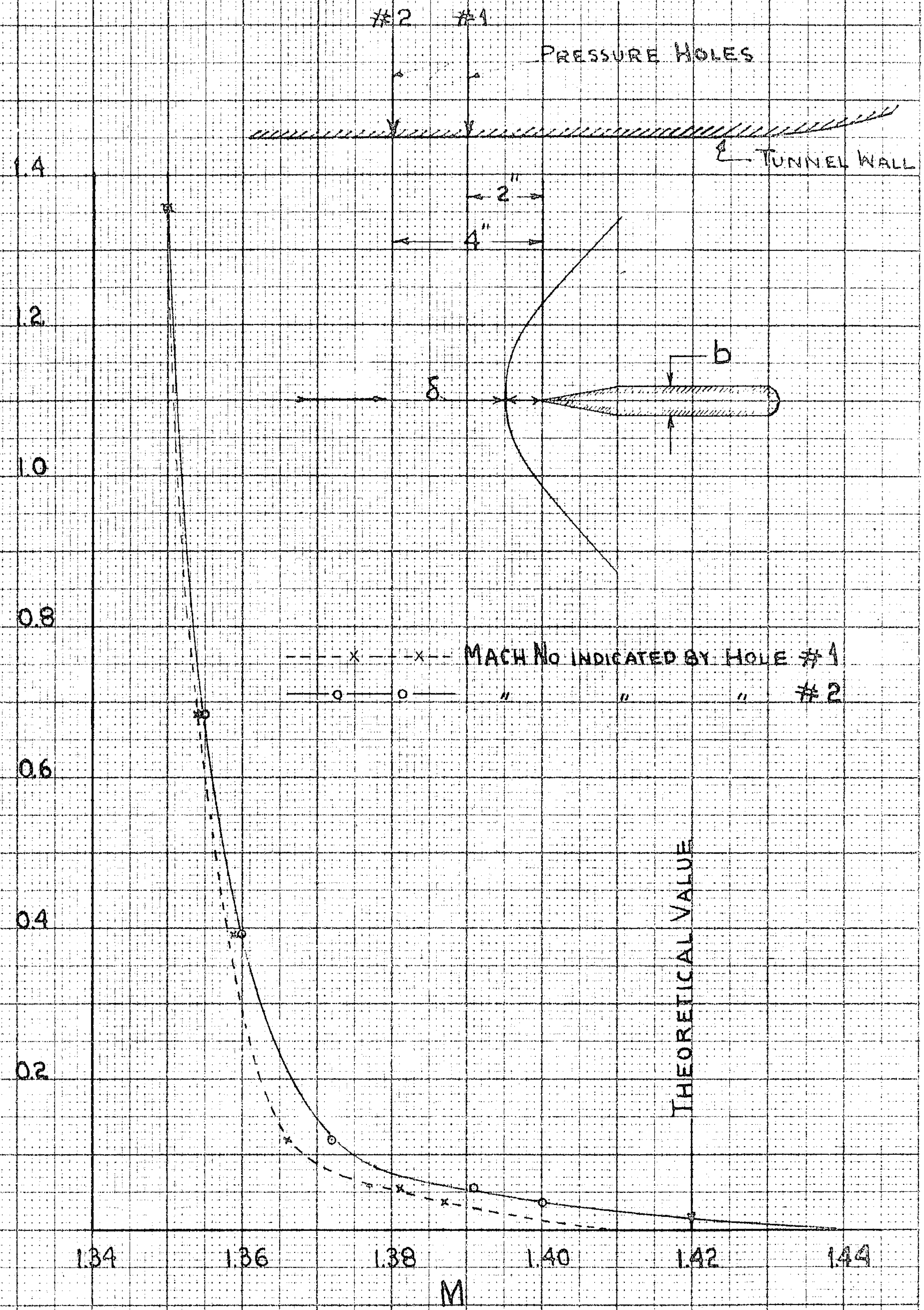

FIG 27

DETACHMENT MACH NUMBER FOR 10° (½ ANGLE) WEDGE